Looking back at EIT brightenings. What is the difference with EUI campfires?

D. Berghmans - ROB/SIDC Seminar 2023 Nov 10 Friday 14:30

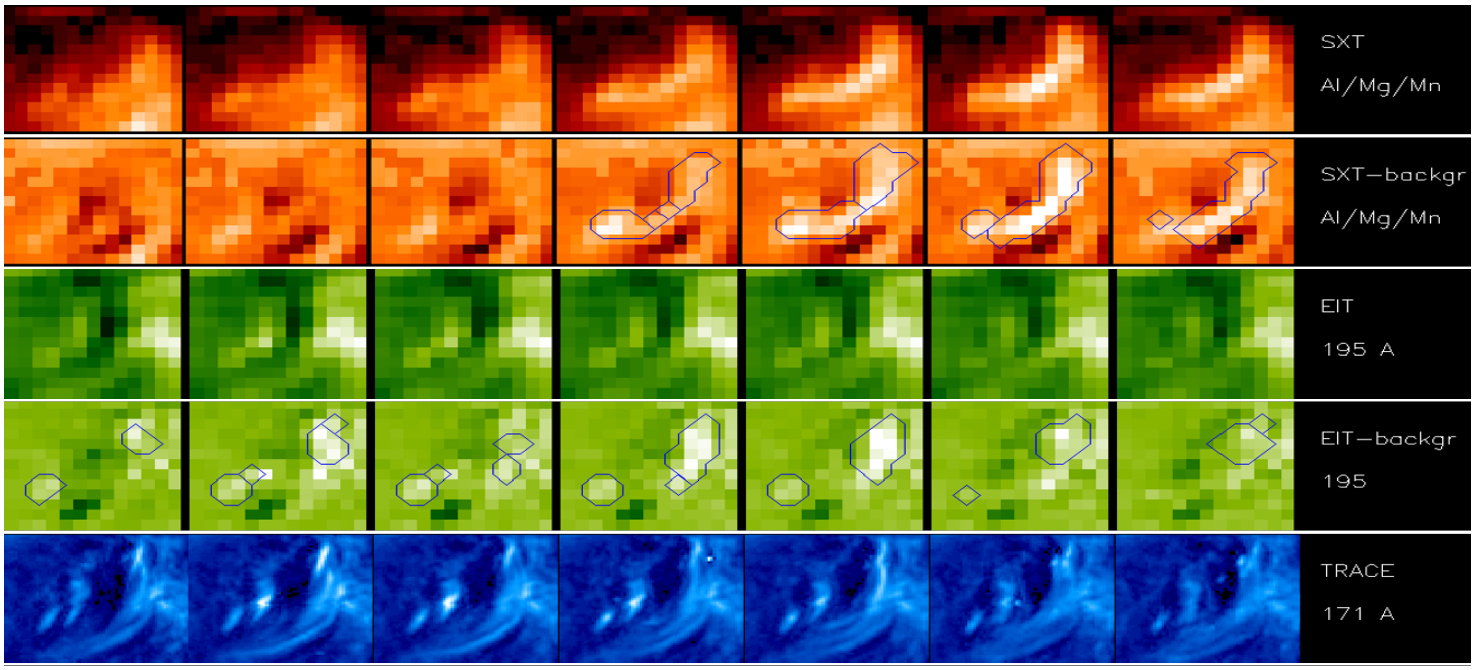

Overview

1. **“Getting hot by Nanoflares”**, Berghmans (2002), ESA SP-506

2. **“Quiet Sun EUV Brightenings”**, Berghmans, Clette, Moses (1998), AA

3. **Linking the old stuff to the new stuff**

Overview

1. **“Getting hot by Nanoflares”**,
   Berghmans (2002), ESA SP-506, ESPM10 Prague

2. **“Quiet Sun EUV Brightenings”**,
   Berghmans, Clette, Moses (1998), AA

3. **Linking the old stuff to the new stuff**

nanoflare statistics

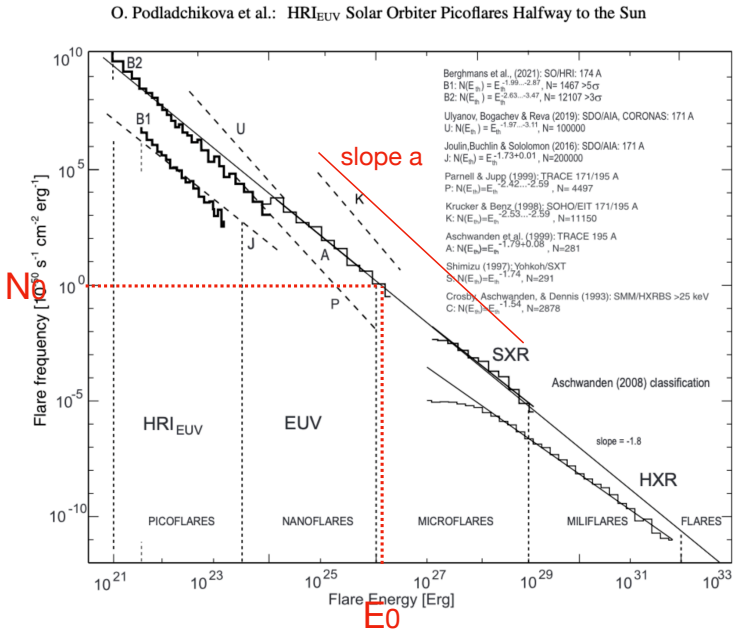

$$N(E)dE = N_0(\frac{E}{E_0})^{-a}.$$

nanoflare statistics

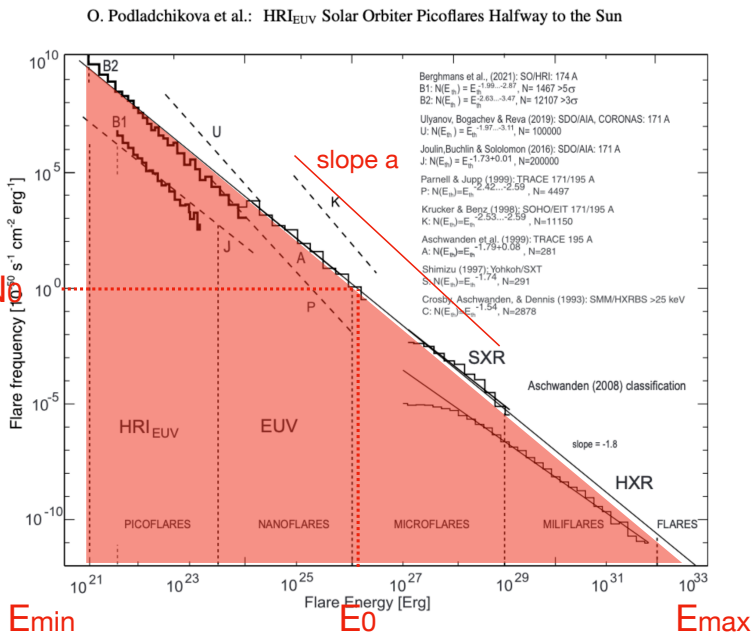

$$N(E)dE = N_0(\frac{E}{E_0})^{-a}.$$

$$W_{tot} = \int_{E_{min}}^{E_{max}} N(E)EdE,$$

$$W_{tot} = \frac{N_0 E_0^2}{(2-a)}[(\frac{E_{max}}{E_0})^{(2-a)} - (\frac{E_{min}}{E_0})^{(2-a)}]$$

$$W_{tot} = \frac{N_0 E_0^2}{(2-a)}[(\frac{E_{max}}{E_0})^{(2-a)} - (\frac{E_{min}}{E_0})^{(2-a)}]$$

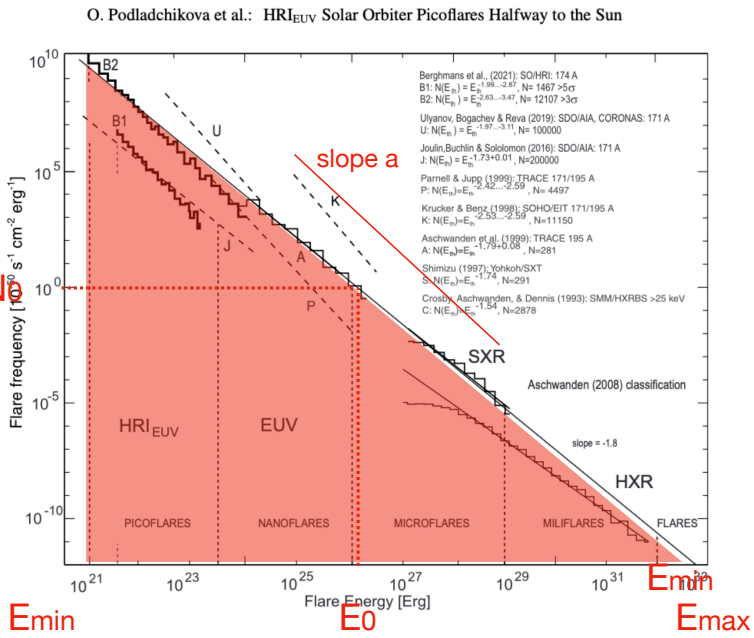

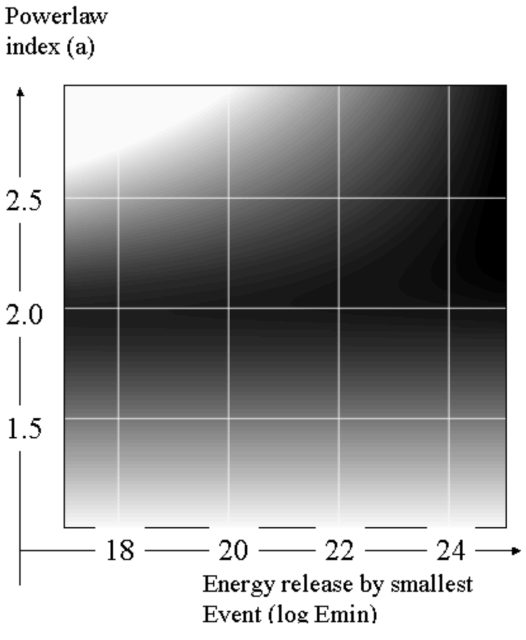

$$W_{tot} = \frac{N_0 E_0^2}{(2-a)}[(\frac{E_{max}}{E_0})^{(2-a)} - (\frac{E_{min}}{E_0})^{(2-a)}]$$

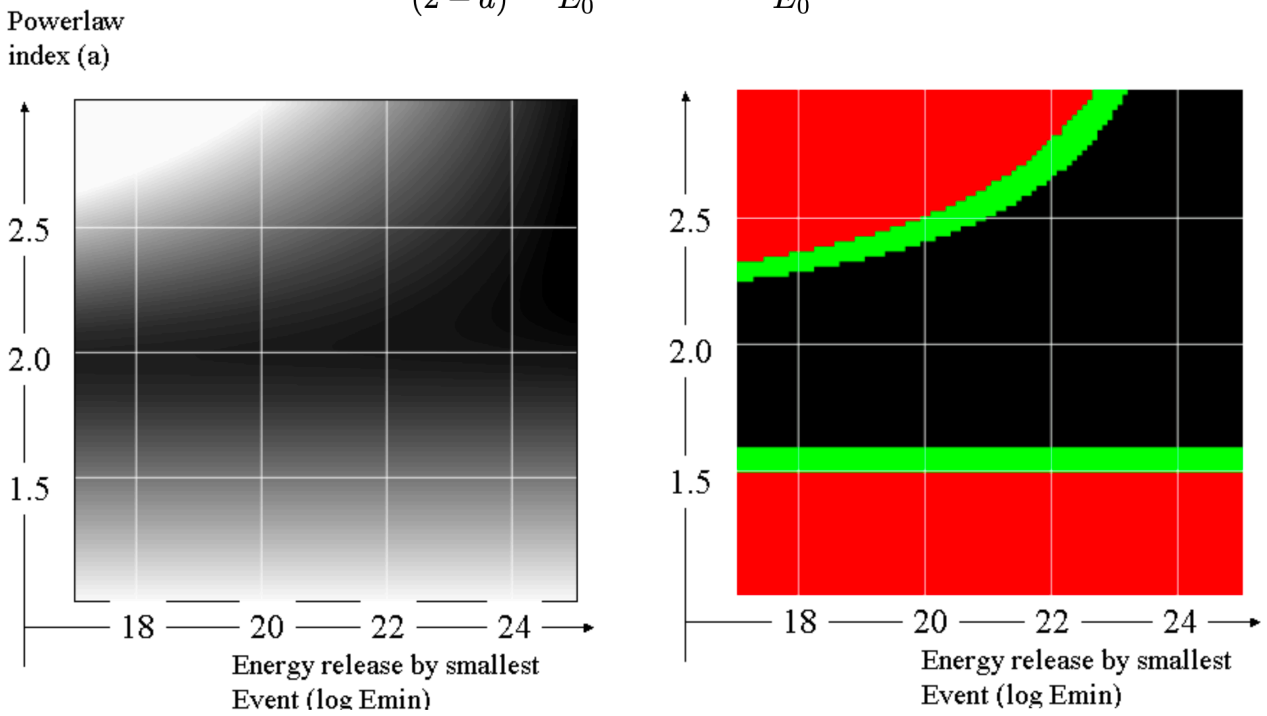

$$W_{tot} = \frac{N_0 E_0^2}{(2-a)}[(\frac{E_{max}}{E_0})^{(2-a)} - (\frac{E_{min}}{E_0})^{(2-a)}]$$

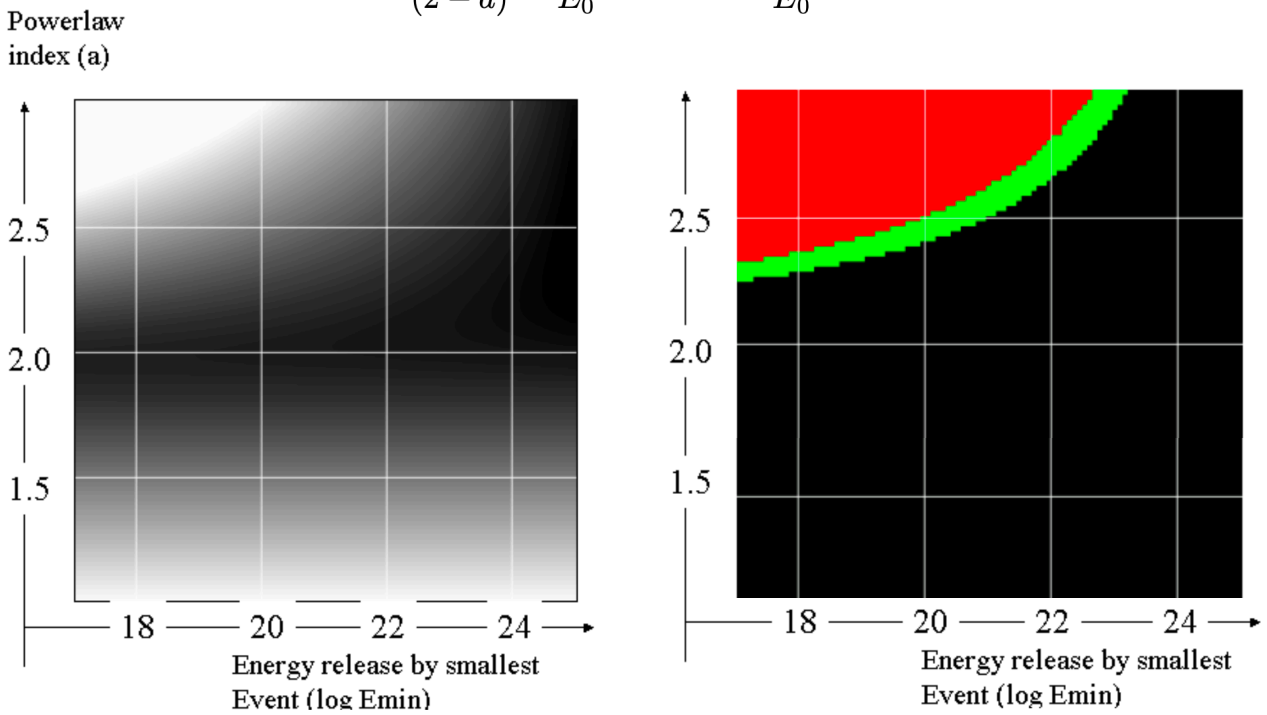

$$W_{tot} = \frac{N_0 E_0^2}{(2-a)}[(\frac{E_{max}}{E_0})^{(2-a)} - (\frac{E_{min}}{E_0})^{(2-a)}]$$

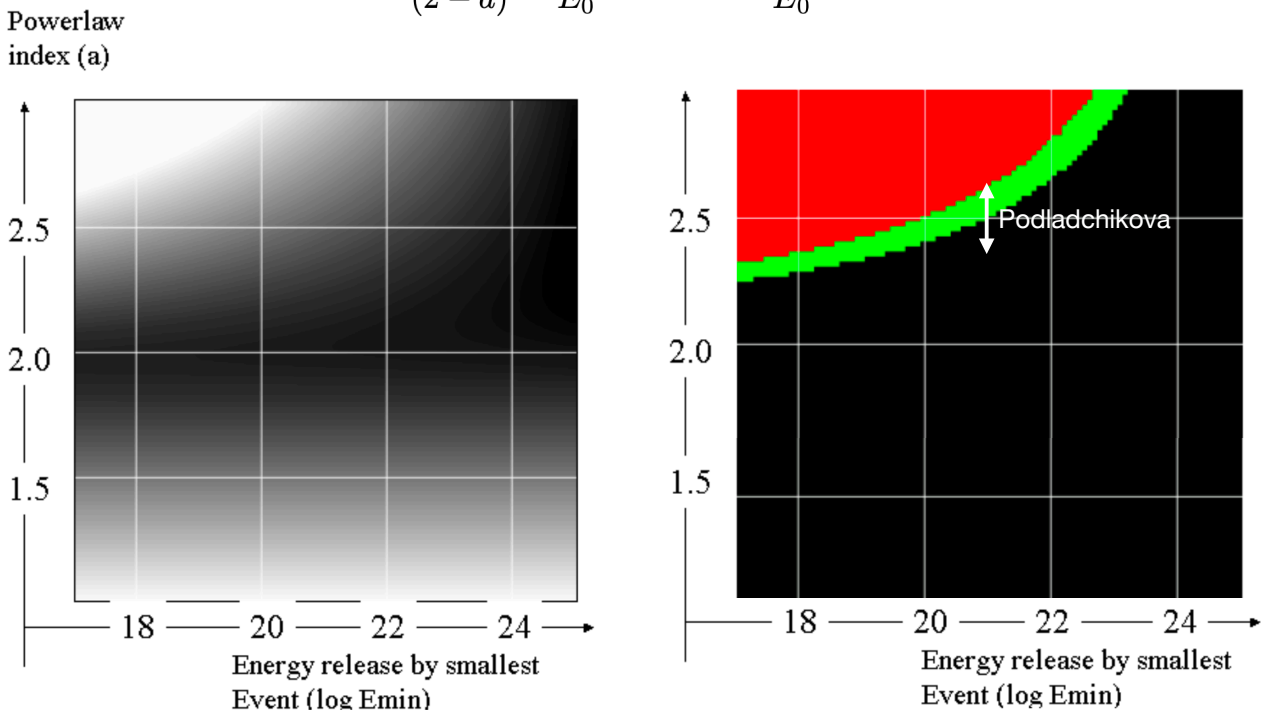

Nanoflare statistics issues

- **choice of wavelength**: lower temperature bandpass will sample more weak events than a hot bandpass
- "**dark" flare power**: part of the flare energy is released before we can see it with EUV imagers, especially for the larger ones
- **grouping of neighbouring events**: being restrictive in spatial grouping leads to increased number of weak events
- **identification of false events:** there is typically higher chance among weak events to be a false identification than among strong events (false = non-flare)
- **energy calculation: (E=n*T*V=n*T*A*l)**
  - **l:** line of sight assumption (constant or sqrt(A)) can lead to a difference of 0.5 on slope
  - **T**: 'filter' peak temperature underestimates temperature most strongly for strongest flares

Last hope for nanoflares?

- E_{th} ~ T^6: smallest flares will liberate their energy at low temperatures
- variability is highest in transition region
- blinkers, explosive events, etc

Explosive events

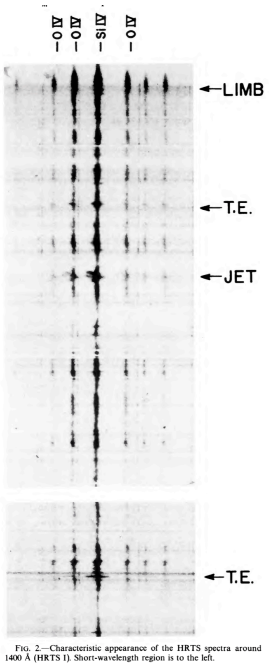

FIG. 2.—Characteristic appearance of the HRTS spectra around 1400 Å (HRTS 1). Short-wavelength region is to the left.

THE ASTROPHYSICAL JOURNAL, 272:329–348, 1983 September 1

OBSERVATIONS OF HIGH-ENERGY JETS IN THE CORONA ABOVE THE QUIET SUN, THE HEATING OF THE CORONA, AND THE ACCELERATION OF THE SOLAR WIND

G. E. BRUECKNER AND J.-D. F. BARTOE
E. O. Hulburt Center for Space Research, Naval Research Laboratory, Washington, D.C.
Received 1982 November 12; accepted 1983 February 11

ABSTRACT

High spatial resolution observations of the ultraviolet solar spectrum reveal high-energy events in the quiet Sun. They can be classified as turbulent events and jets. The turbulent events show high turbulence (up to 250 km s^{-1}) confined in small areas ($<2''$), while the jets show upward moving material with velocities ($\sim$400 km s^{-1}) exceeding the sound velocity ($\sim$120 km s^{-1}) in the corona. A single jet carries an energy of 2.5×10^{26} ergs and a mass of 3×10^{11} g at 400 km s^{-1} into the corona at an altitude of 4000–16,000 km. Strong shock waves accompanying the jets can heat the corona. A cloud model of the solar wind is proposed where all the kinetic energy of the wind is provided at the solar surface by the high-energy jets. With a birthrate of 24 events per second over the whole Sun, which is within the uncertainties of the observations, the power (6×10^{27} ergs s^{-1}) and mass flux (2×10^{12} g s^{-1}) requirements of the corona and the solar wind can be satisfied. The acceleration of the jets is 5 km s^{-2} and constant during their maximum

Explosive events

O IV (1.3×10^5 K) and Si IV (8×10^4 K)

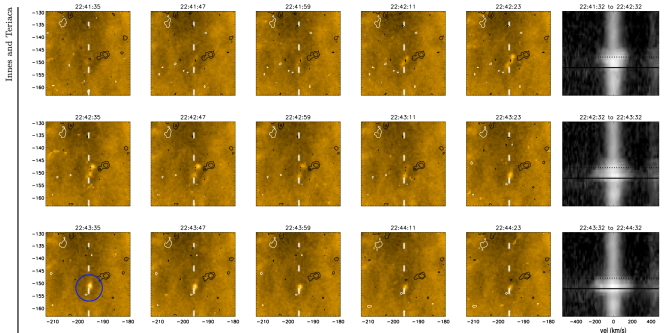

Figure 4.: The five 171Å AIA images along each row shows the evolution during the SUMER O VI exposure on the right. The vertical light blue dashed line in the middle of each 171Å image indicates the position of the SUMER slit. Line-of-sight magnetic field contours at +/-20, 50 G are overplotted in white/black. On the SUMER spectra horizontal black solid and dotted lines indicate the position of the profiles shown in Figure 5. The blue circle in the bottom row surrounds the 'splash'.

Innes and Teriaca, 2012

Table 4. The properties of UV explosive events due to Innes et al. (1997).

Property	Value
Global frequency	500 s^{-1}
Velocity	150 km s^{-1}
Area	2.3×10^6 km^2
Mean Lifetime	60 s

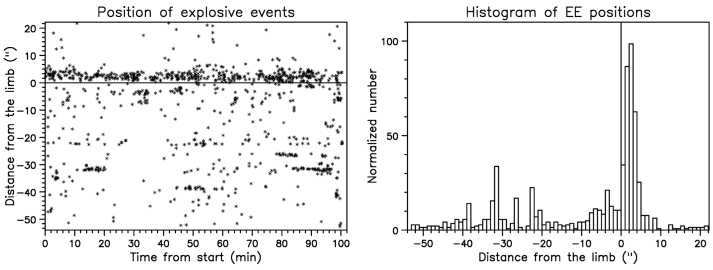

Allesandrakis & Vial, 2023

Blinkers

EUV BLINKERS:
THE SIGNIFICANCE OF VARIATIONS
IN THE EXTREME ULTRAVIOLET QUIET SUN

RICHARD A. HARRISON
Space Science Department, Rutherford Appleton Laboratory, Chilton, Didcot, Oxfordshire OX11 0QX, U.K.

(Received 8 January 1997; accepted 12 June 1997)

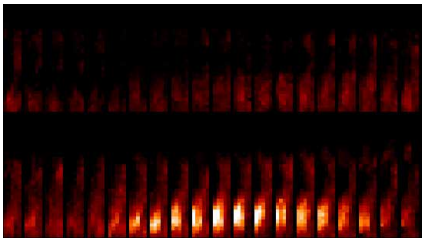

Table 1. The properties of EUV blinkers due to Bewsher et al. (2002).

Property	Value
Global frequency	10–20 s^{-1}
Mean intensity enhancement (O V)	70–80%
Mean Area	$2–3 \times 10^7$ km^2
Mean Lifetime	16.4 min

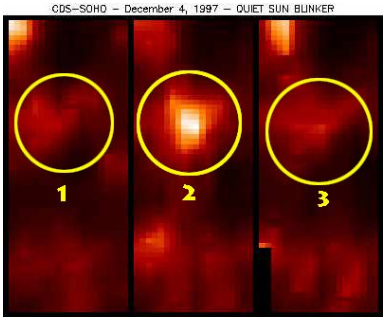

Astronomy & Astrophysics manuscript no. blinkers˙fin
October 11, 2018

What is the true nature of blinkers?

S. Subramanian[1], M. S. Madjarska[1], J. G. Doyle[1] and D. Bewsher[2]

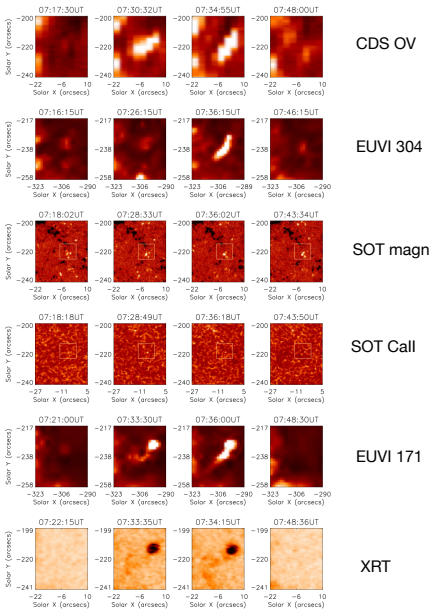

Fig. 2: Blinker group 1 from top in CDS O v 629 Å, EUVI 304 Å, SOT FG magnetograms, SOT Ca II H, EUVI 171 Å and XRT Al_poly. The corresponding magnetogram field-of-view from which the lightcurve of the positive flux was derived, is outlined by the white box on the SOT FG magnetograms and Ca II H images.

Overview

1. **“Getting hot by Nanoflares”**,
   Berghmans (2002), ESA SP-506, ESPM10 Prague

2. **“Quiet Sun EUV Brightenings”**,
   Berghmans, Clette, Moses (1998), AA

3. **Linking the old stuff to the new stuff**

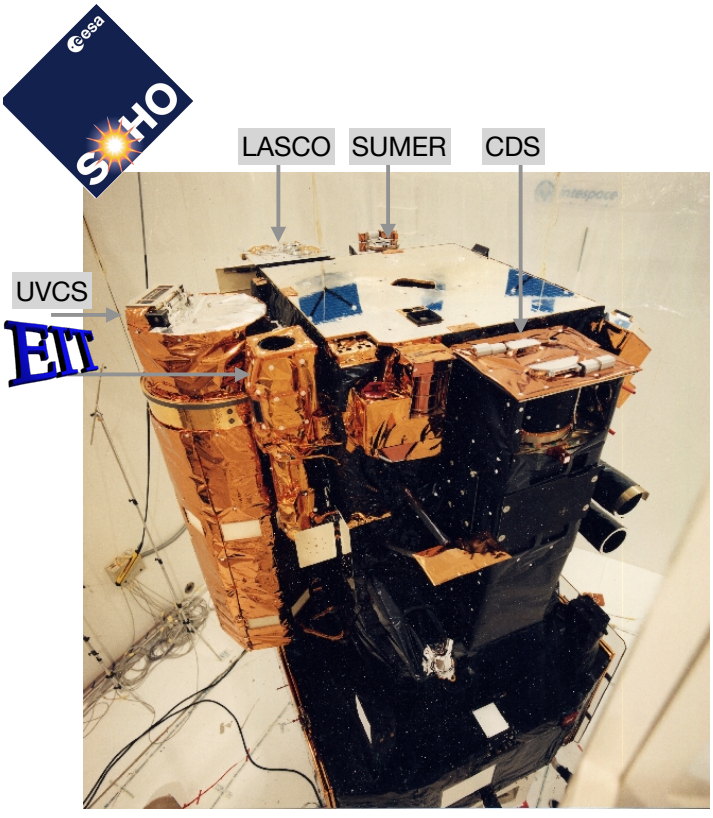

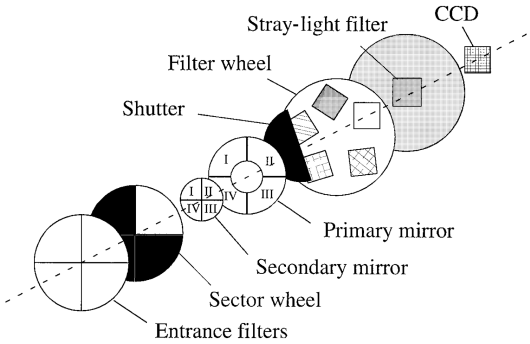

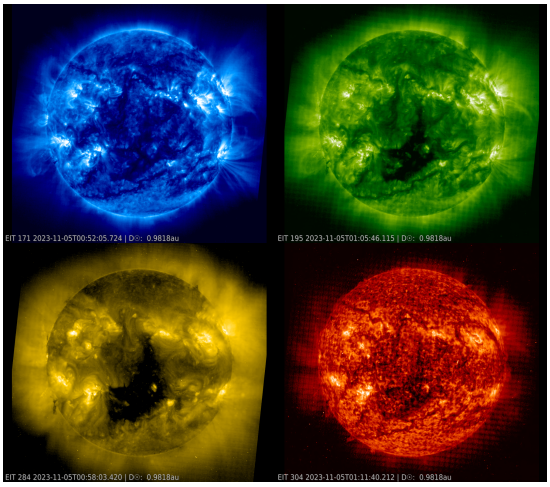

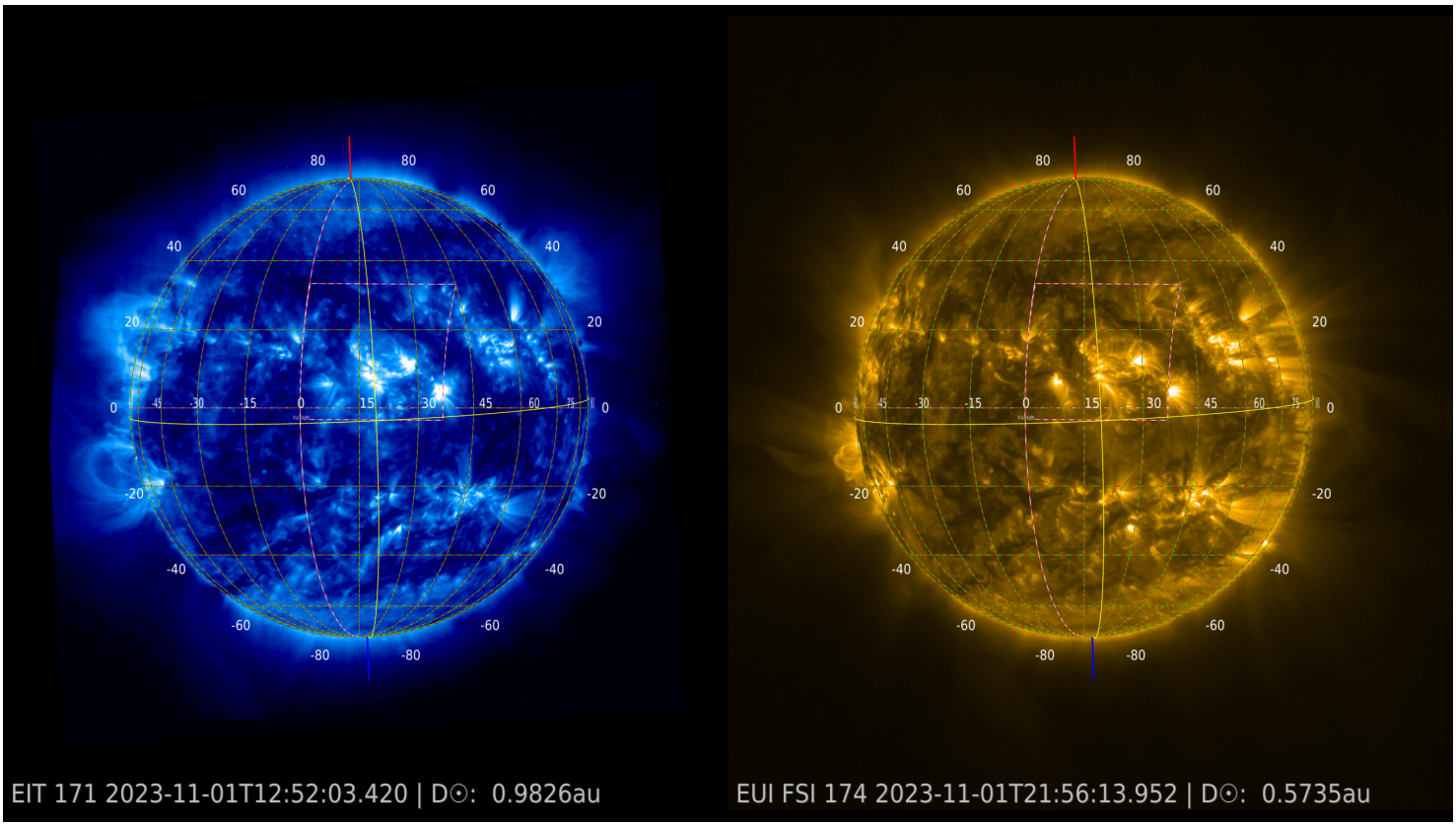
EIT 171 2023-11-01T12:52:03.420 | D☉: 0.9826au
EUI FSI 174 2023-11-01T21:56:13.952 | D☉: 0.5735au

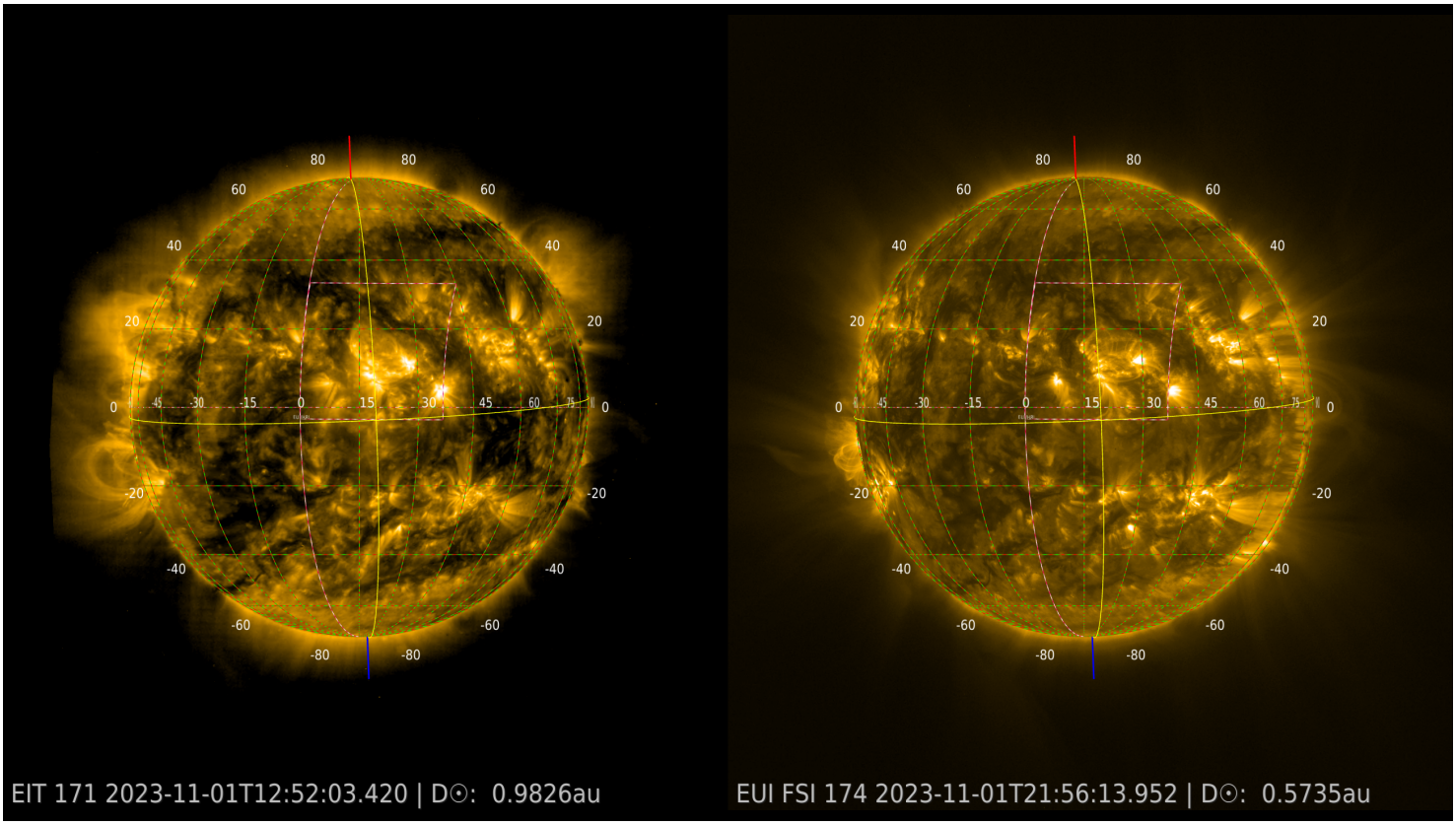
EIT 171 2023-11-01T12:52:03.420 | D☉: 0.9826au
EUI FSI 174 2023-11-01T21:56:13.952 | D☉: 0.5735au

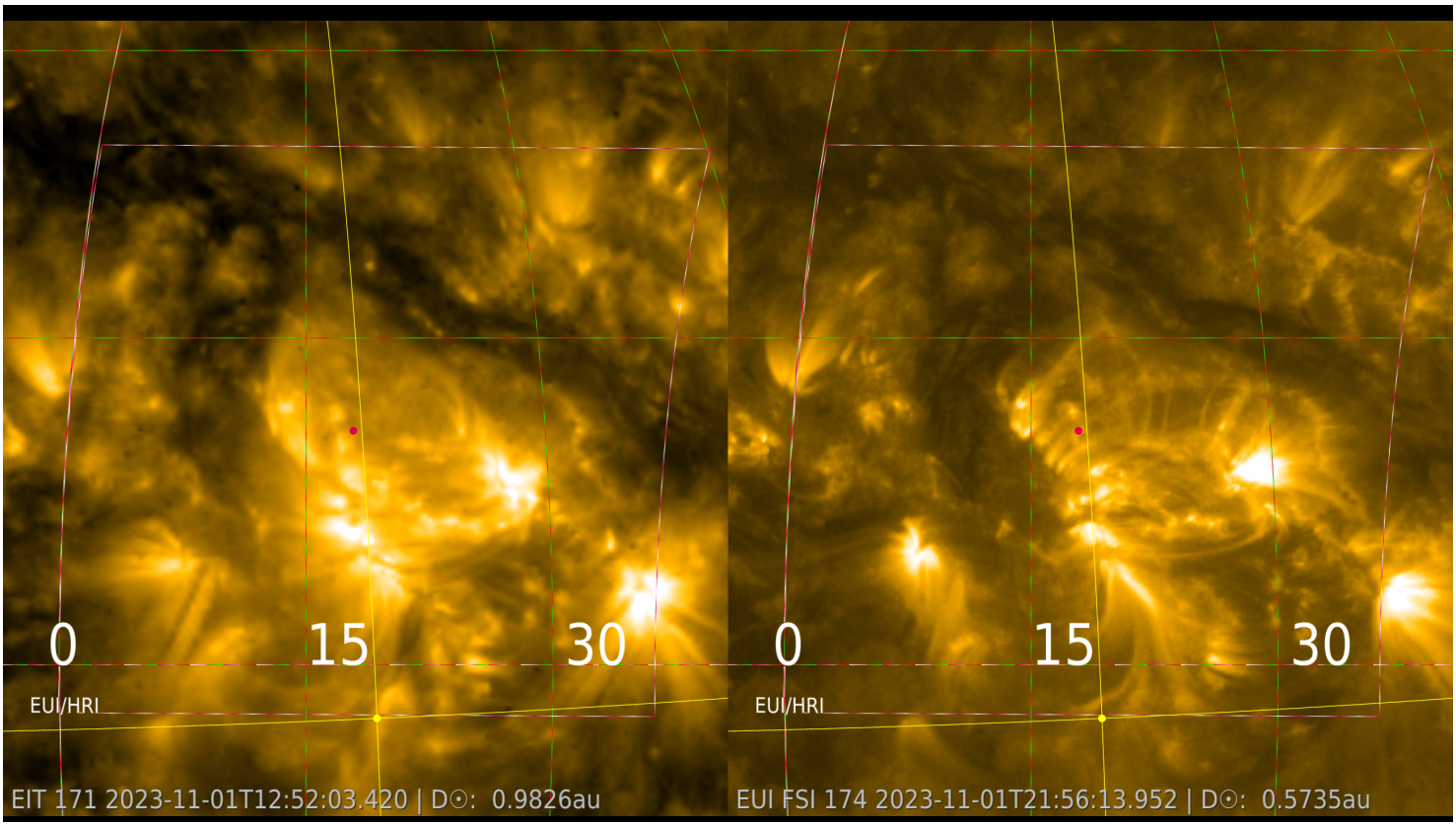
0
15
30
EUI/HRI
EIT 171 2023-11-01T12:52:03.420 | D☉: 0.9826au
0
15
30
EUI/HRI
EUI FSI 174 2023-11-01T21:56:13.952 | D☉: 0.5735au

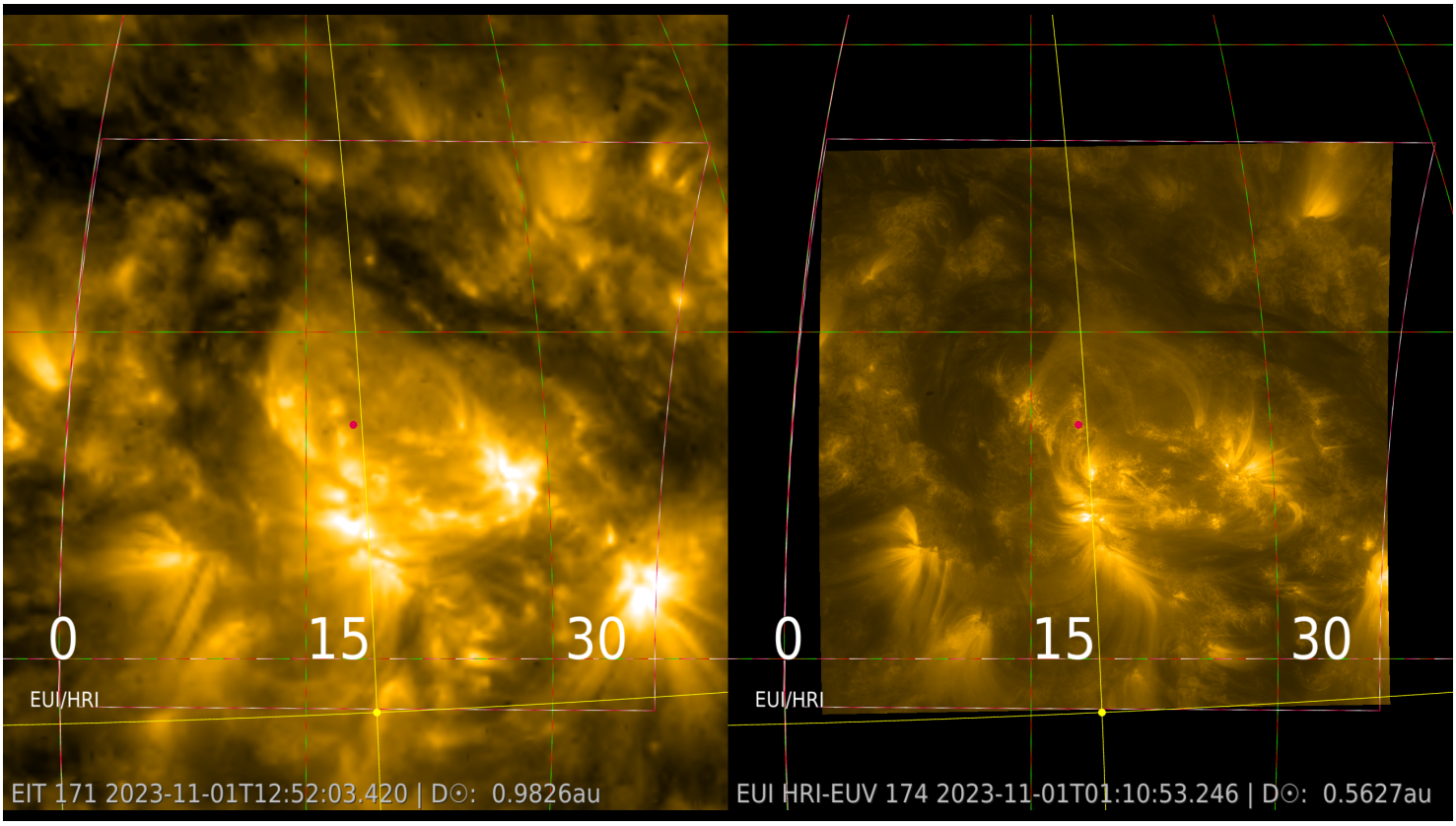
0
15
30
EUI/HRI
EIT 171 2023-11-01T12:52:03.420 | D☉: 0.9826au
0
15
30
EUI/HRI
EUI HRI-EUV 174 2023-11-01T01:10:53.246 | D☉: 0.5627au

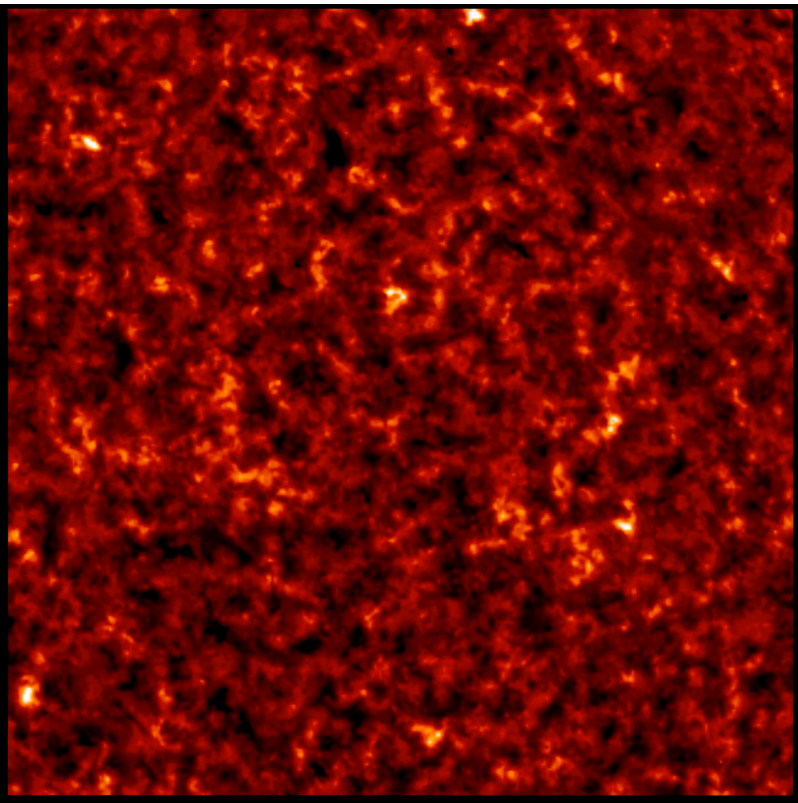

EIT He II 30.4nm ~ 80000K peak formation T

320x 320 pixels, 2.62”/pix = 1890 km/pix

173 images, 1 image per min

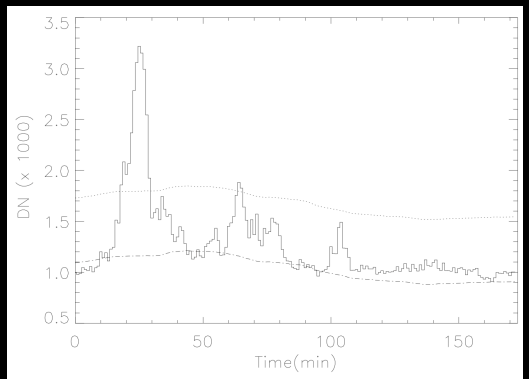

Fig. 12. Example of a light curve (solid line) of a single pixel in the transition region sequence. This somewhat special pixel was selected for the succession of a large brightening ($t = 25$ min), a more average brightening ($t = 65$ min), a small brightening that escaped detection ($t = 105$ min) and small variability in agreement with the expected photon shot noise ($t = 140$ min). As a reference we also provide the calculated -see Sect. 4.1- background intensity (dot-dashed line) and the $\Sigma_P = 3\ \sigma_{ov}$ level (detection limit, dotted line).

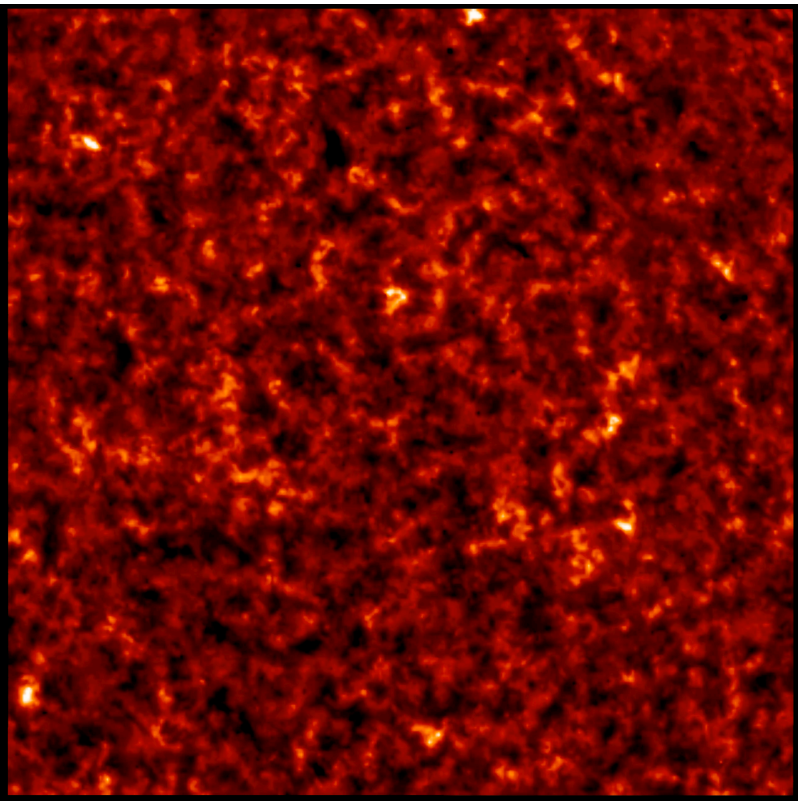

Table 4. Number of events detected at a peak threshold Σ_P and with an edge threshold Σ_E. Only events which have their full duration within the sequence length and which are not adjacent to image edges are counted in the third column.

Σ_P	Σ_E	number of events detected	full Sun birthrate
$5\ \sigma_{ov}$	$2\ \sigma_{ov}$	188	0.3/s
$4\ \sigma_{ov}$	$2\ \sigma_{ov}$	1473	2.4/s
$3\ \sigma_{ov}$	$2\ \sigma_{ov}$	9187	14.4/s
$2.5\ \sigma_{ov}$	$1.5\ \sigma_{ov}$	13067	19.9/s

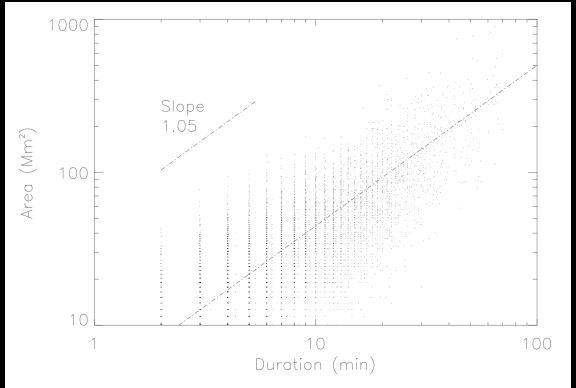

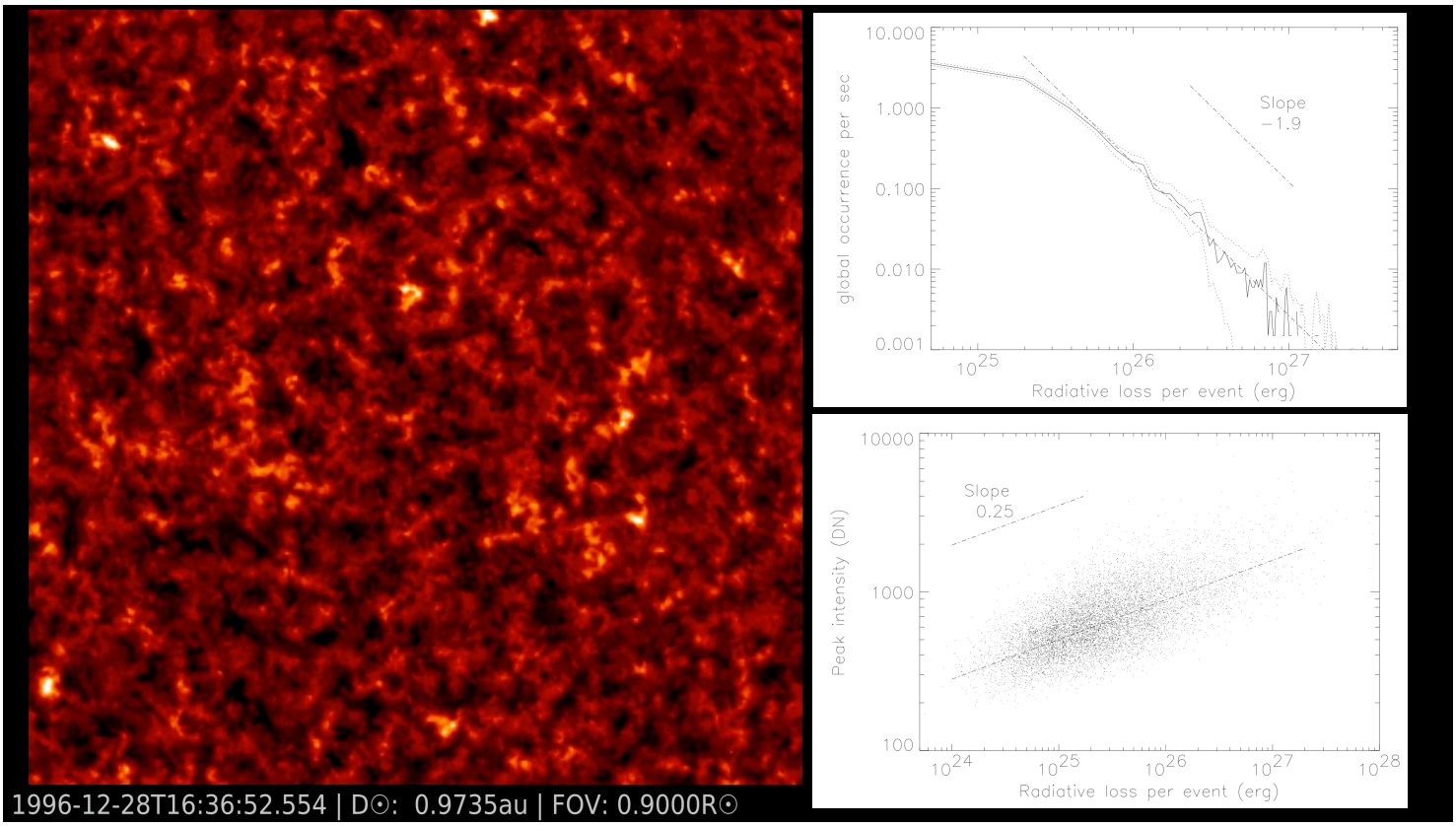
1996-12-28T16:36:52.554 | D⊙: 0.9735au | FOV: 0.9000R⊙
10.000
1.000
0.100
0.010
0.001
global occurrence per sec
Slope
−1.9
10^{25}
10^{26}
10^{27}
Radiative loss per event (erg)
10000
1000
100
Peak intensity (DN)
Slope
0.25
10^{24}
10^{25}
10^{26}
10^{27}
10^{28}
Radiative loss per event (erg)

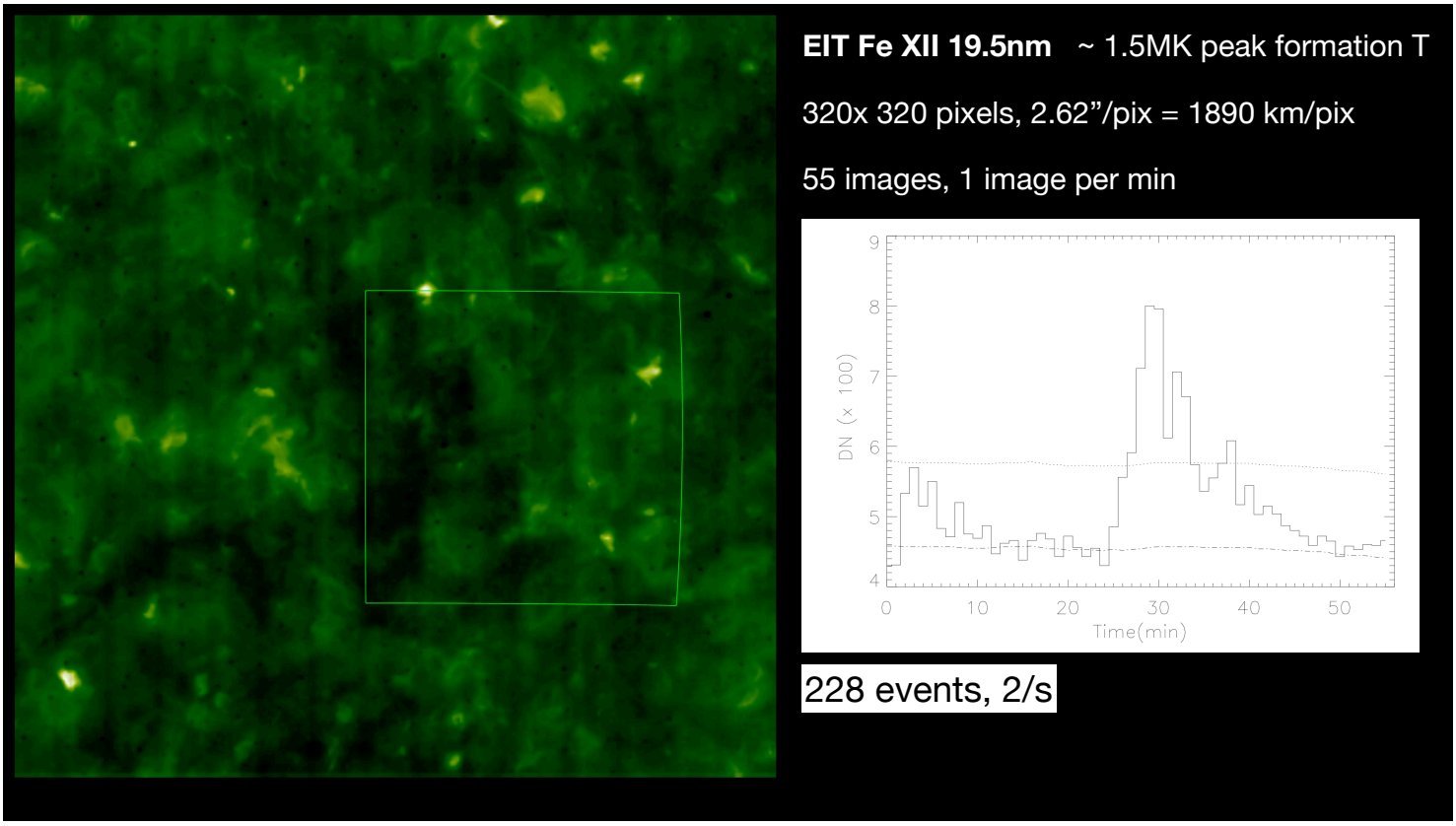
EIT Fe XII 19.5nm ~ 1.5MK peak formation T
320x 320 pixels, 2.62”/pix = 1890 km/pix
55 images, 1 image per min
9
8
7
6
5
4
DN (× 100)
0
10
20
30
40
50
Time(min)
228 events, 2/s

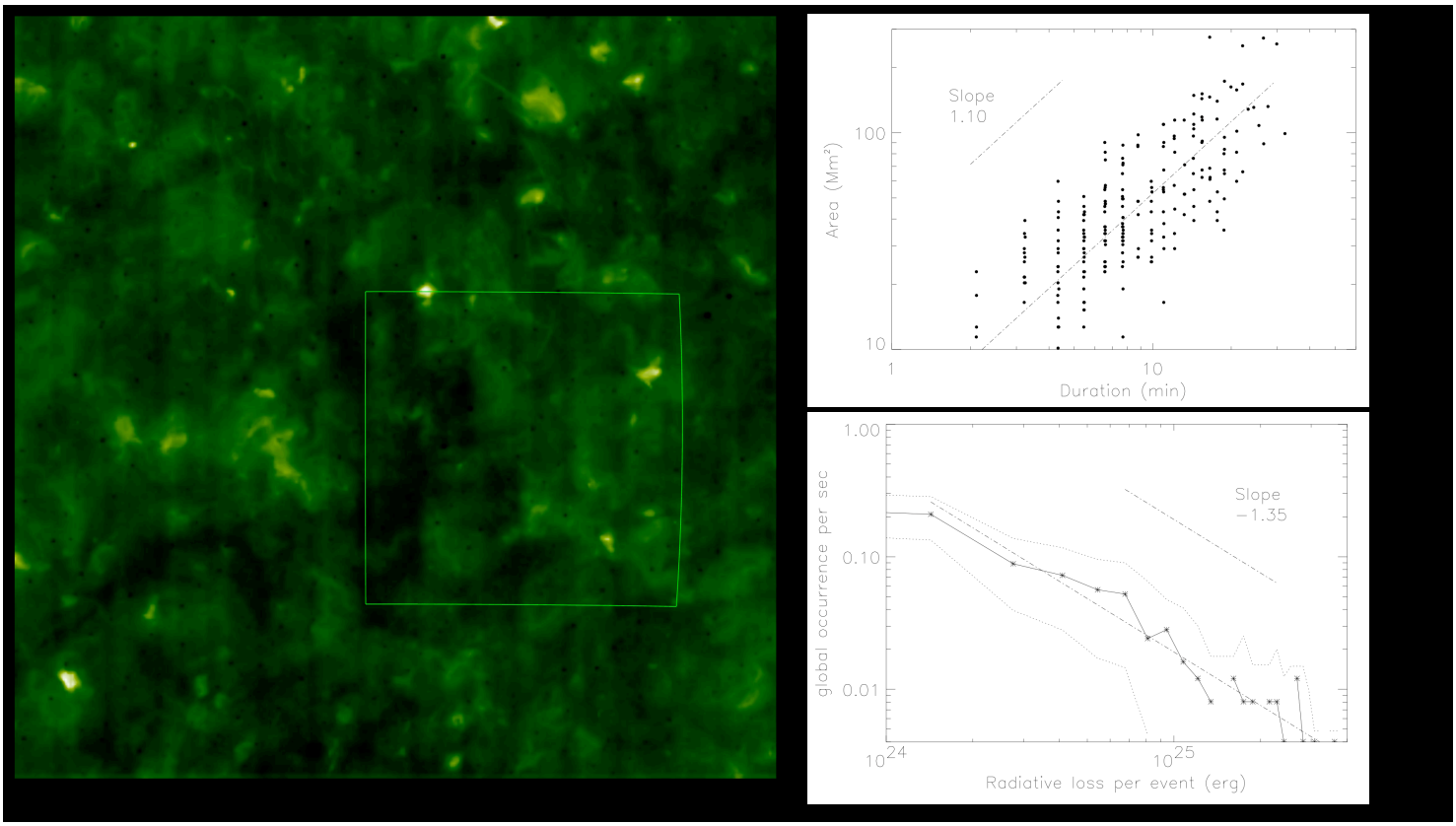

Overview

1. **“Getting hot by Nanoflares”**,
   Berghmans (2002), ESA SP-506, ESPM10 Prague

2. **“Quiet Sun EUV Brightenings”**,
   Berghmans, Clette, Moses (1998), AA

3. **Linking the old stuff to the new stuff**

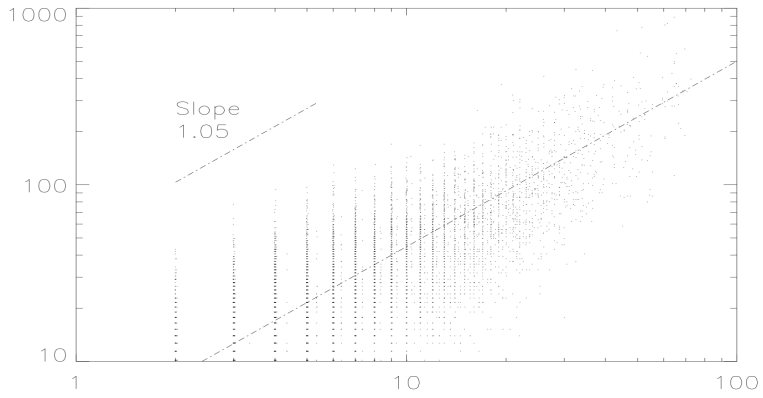
1000
100
10
1
10
100
Slope
1.05

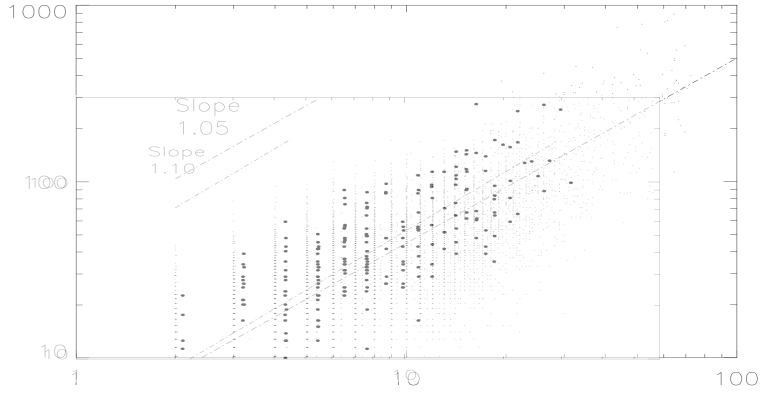
1000
100
10
1
10
100
Slope
1.05
Slope
1.10

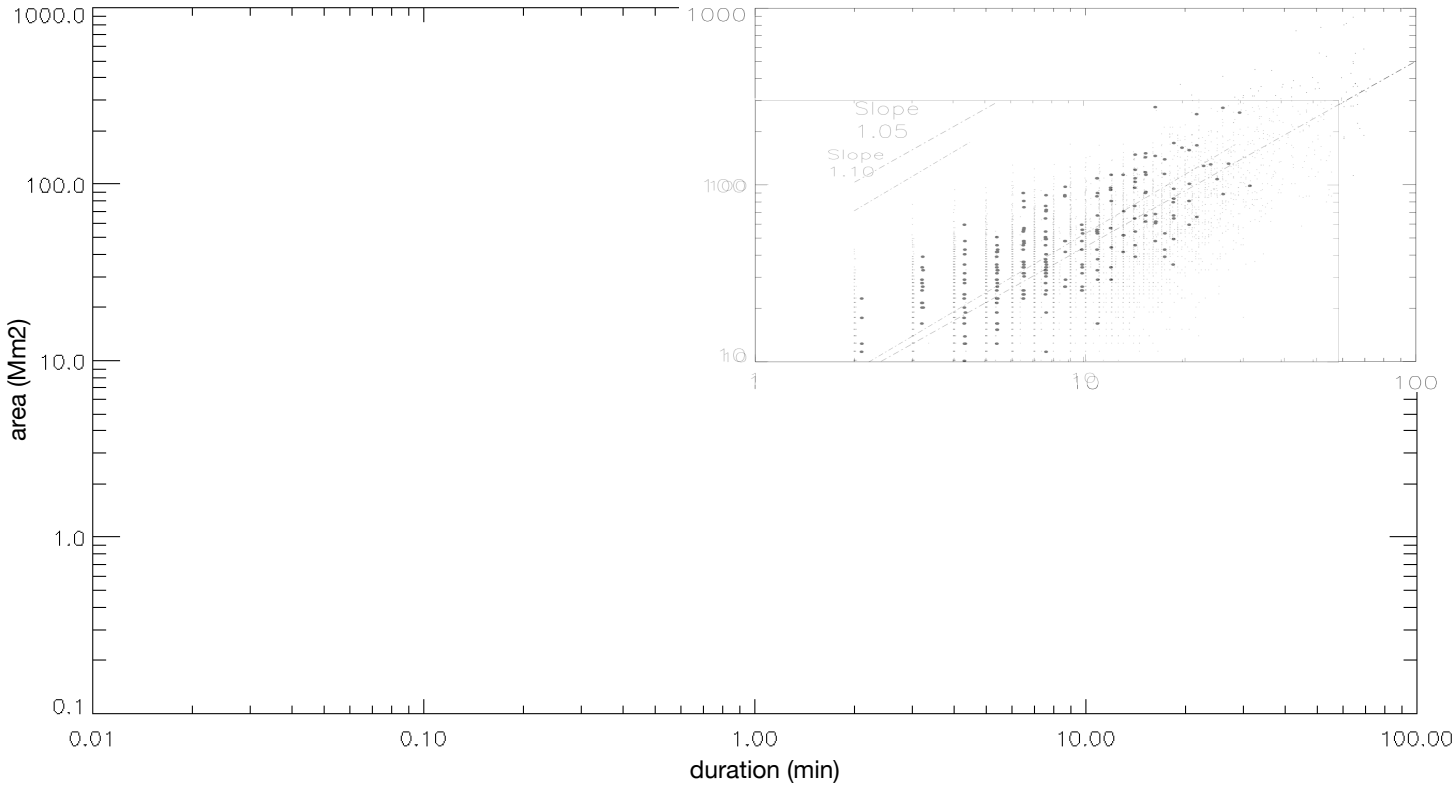
1000.0
100.0
10.0
1.0
0.1
area (Mm2)
0.01
0.10
1.00
10.00
100.00
duration (min)
1000
100
10
1
10
100
Slope
1.05
Slope
1.10

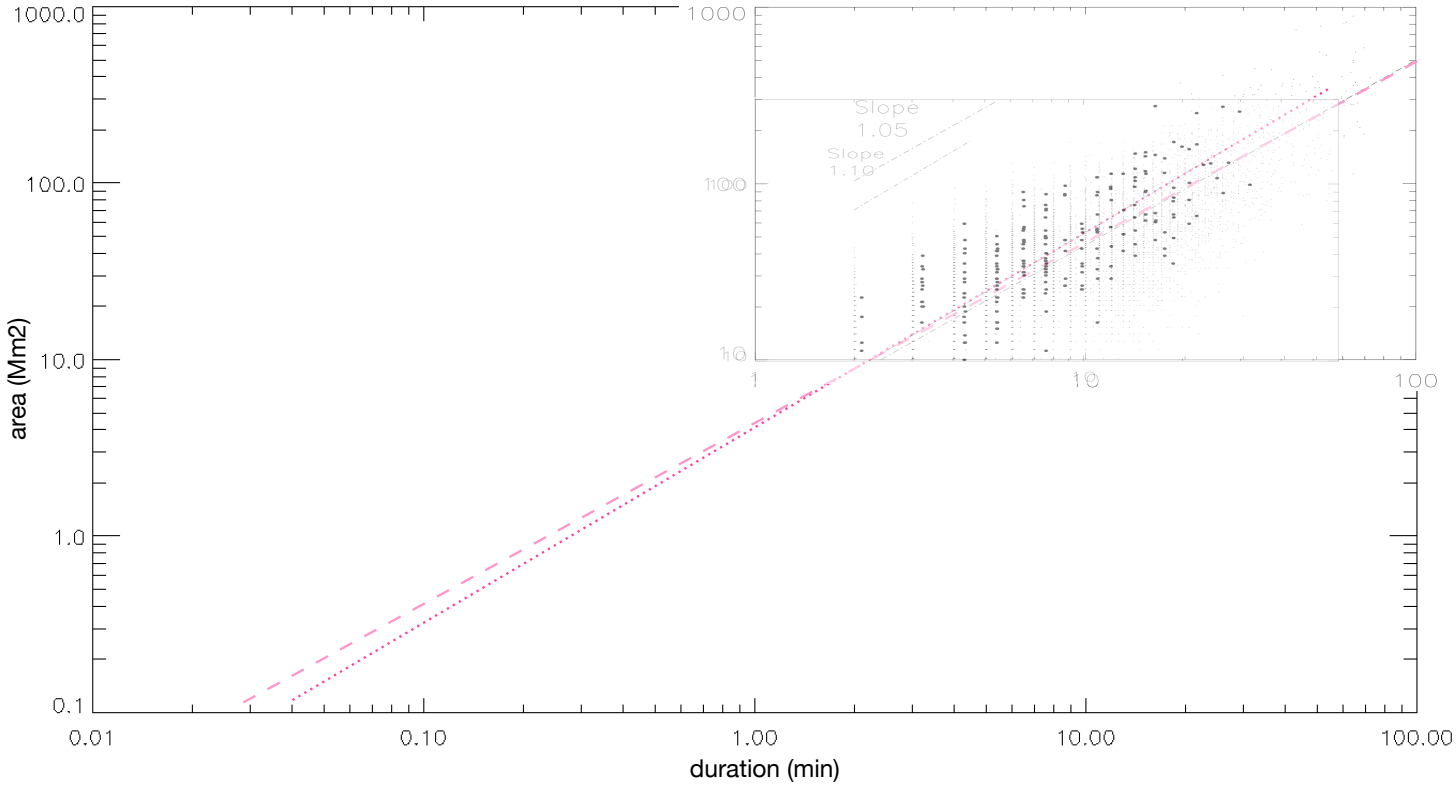
1000.0
100.0
10.0
1.0
0.1
area (Mm2)
0.01
0.10
1.00
10.00
100.00
duration (min)
1000
100
10
1
10
100
Slope
1.05
Slope
1.10

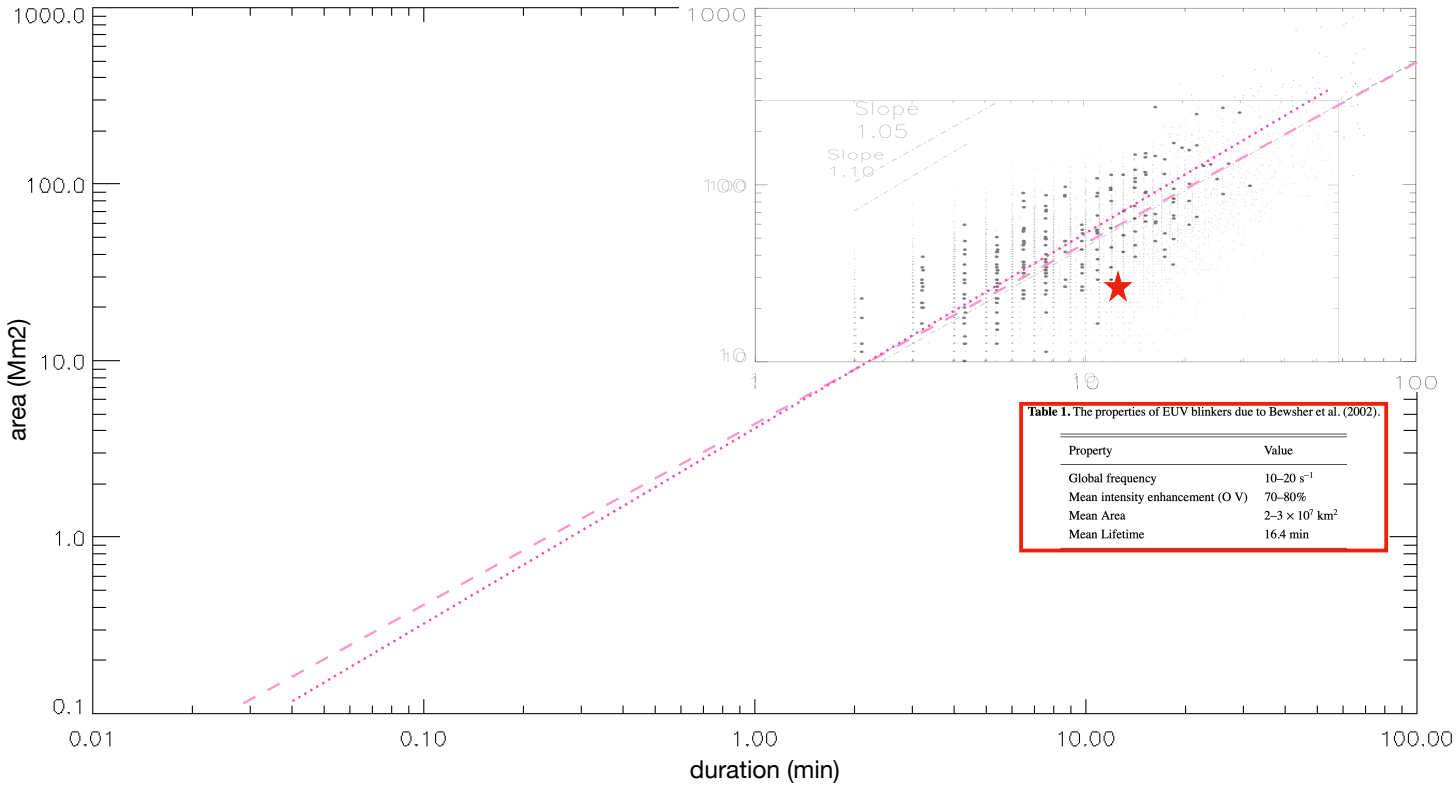

Table 1. The properties of EUV blinkers due to Bewsher et al. (2002).

Property	Value
Global frequency	10–20 s^{-1}
Mean intensity enhancement (O V)	70–80%
Mean Area	2–3 × 10^7 km^2
Mean Lifetime	16.4 min

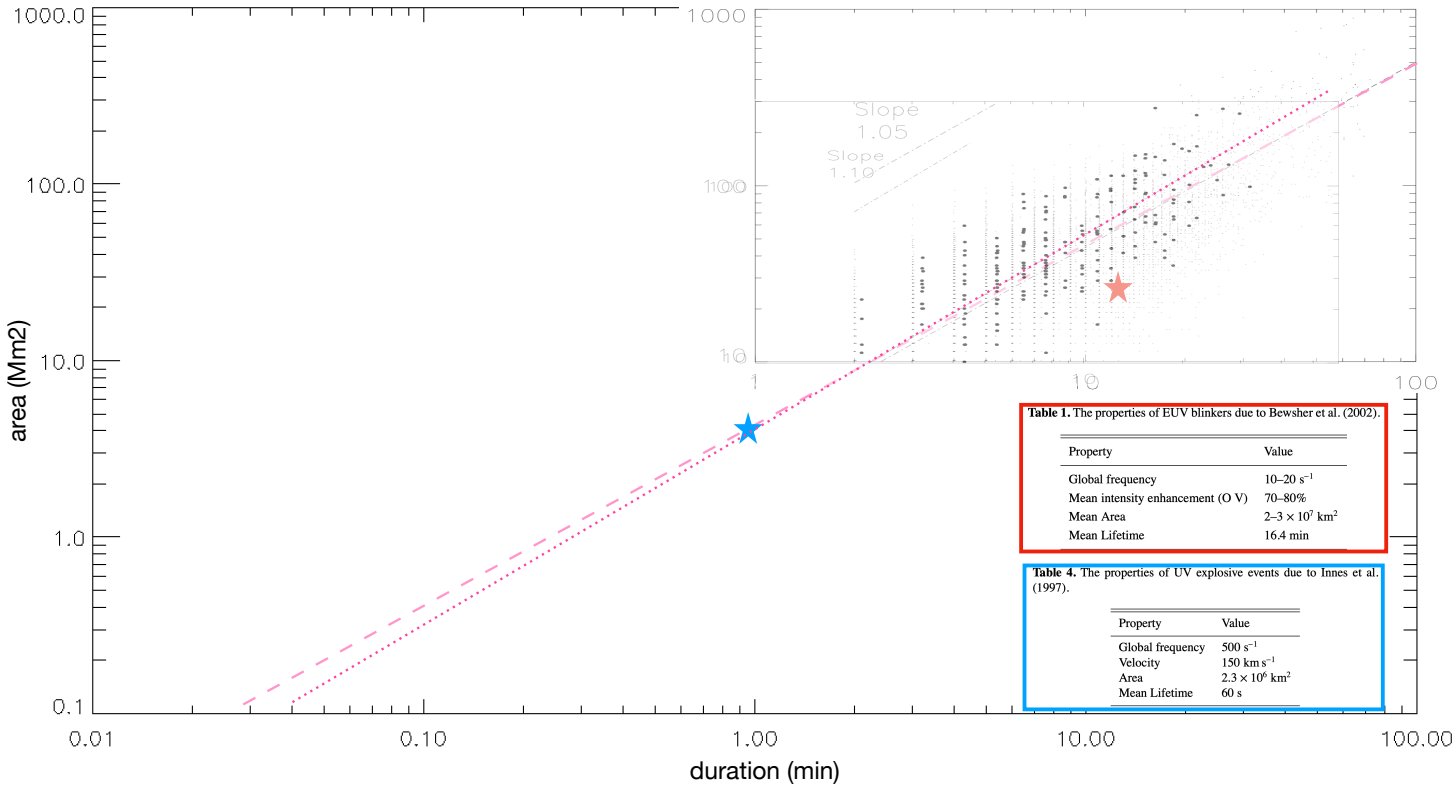

Table 1. The properties of EUV blinkers due to Bewsher et al. (2002).

Property	Value
Global frequency	10–20 s^{-1}
Mean intensity enhancement (O V)	70–80%
Mean Area	2–3 × 10^7 km^2
Mean Lifetime	16.4 min

Table 4. The properties of UV explosive events due to Innes et al. (1997).

Property	Value
Global frequency	500 s^{-1}
Velocity	150 km s^{-1}
Area	2.3 × 10^6 km^2
Mean Lifetime	60 s

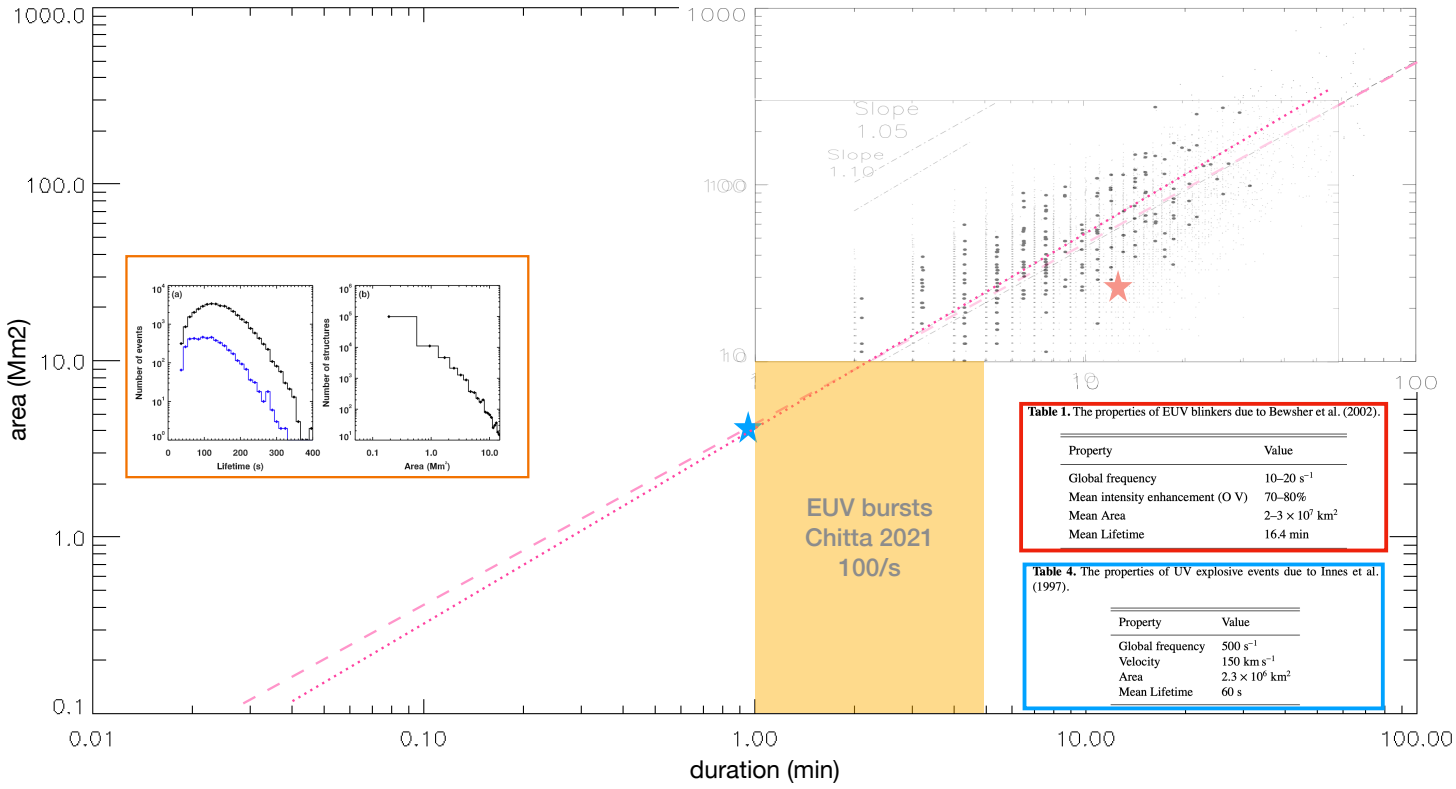

Table 1. The properties of EUV blinkers due to Bewsher et al. (2002).

Property	Value
Global frequency	10–20 s^{-1}
Mean intensity enhancement (O V)	70–80%
Mean Area	2–3 × 10^7 km^2
Mean Lifetime	16.4 min

Table 4. The properties of UV explosive events due to Innes et al. (1997).

Property	Value
Global frequency	500 s^{-1}
Velocity	150 km s^{-1}
Area	2.3 × 10^6 km^2
Mean Lifetime	60 s

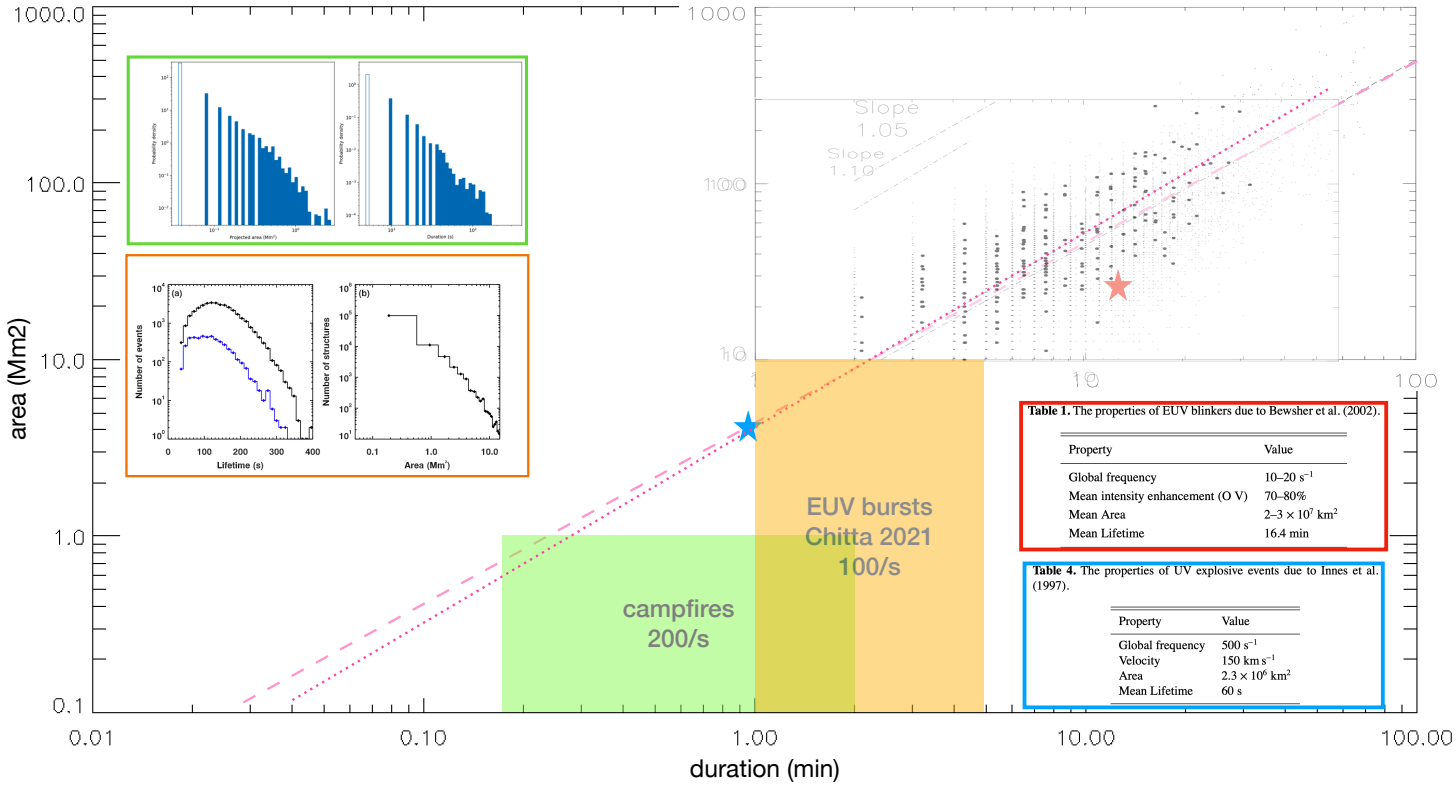

Table 1. The properties of EUV blinkers due to Bewsher et al. (2002).

Property	Value
Global frequency	10–20 s^{-1}
Mean intensity enhancement (O V)	70–80%
Mean Area	2–3 × 10^7 km^2
Mean Lifetime	16.4 min

Table 4. The properties of UV explosive events due to Innes et al. (1997).

Property	Value
Global frequency	500 s^{-1}
Velocity	150 km s^{-1}
Area	2.3 × 10^6 km^2
Mean Lifetime	60 s

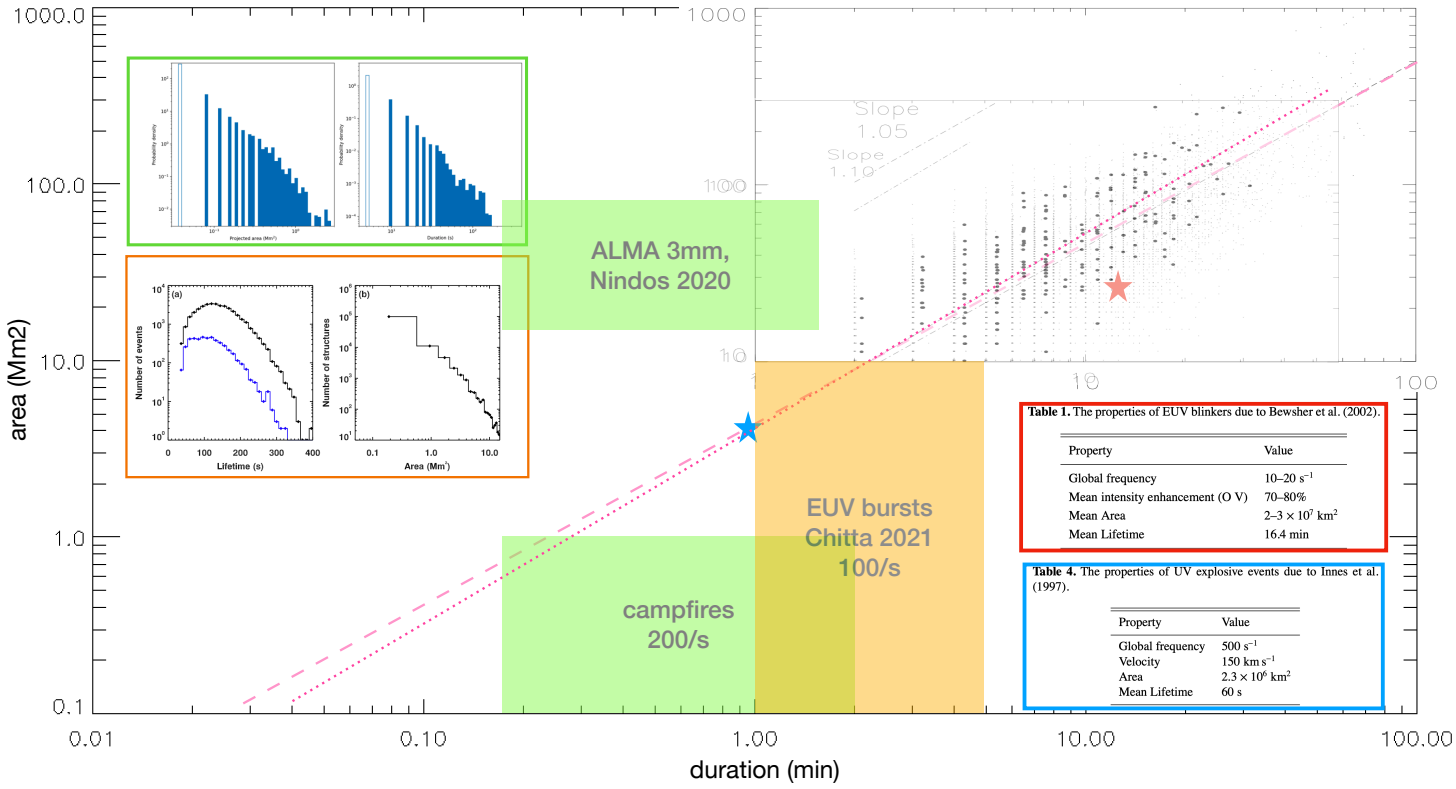

Table 1. The properties of EUV blinkers due to Bewsher et al. (2002).

Property	Value
Global frequency	10–20 s^{-1}
Mean intensity enhancement (O V)	70–80%
Mean Area	2–3 × 10^7 km^2
Mean Lifetime	16.4 min

Table 4. The properties of UV explosive events due to Innes et al. (1997).

Property	Value
Global frequency	500 s^{-1}
Velocity	150 km s^{-1}
Area	2.3 × 10^6 km^2
Mean Lifetime	60 s

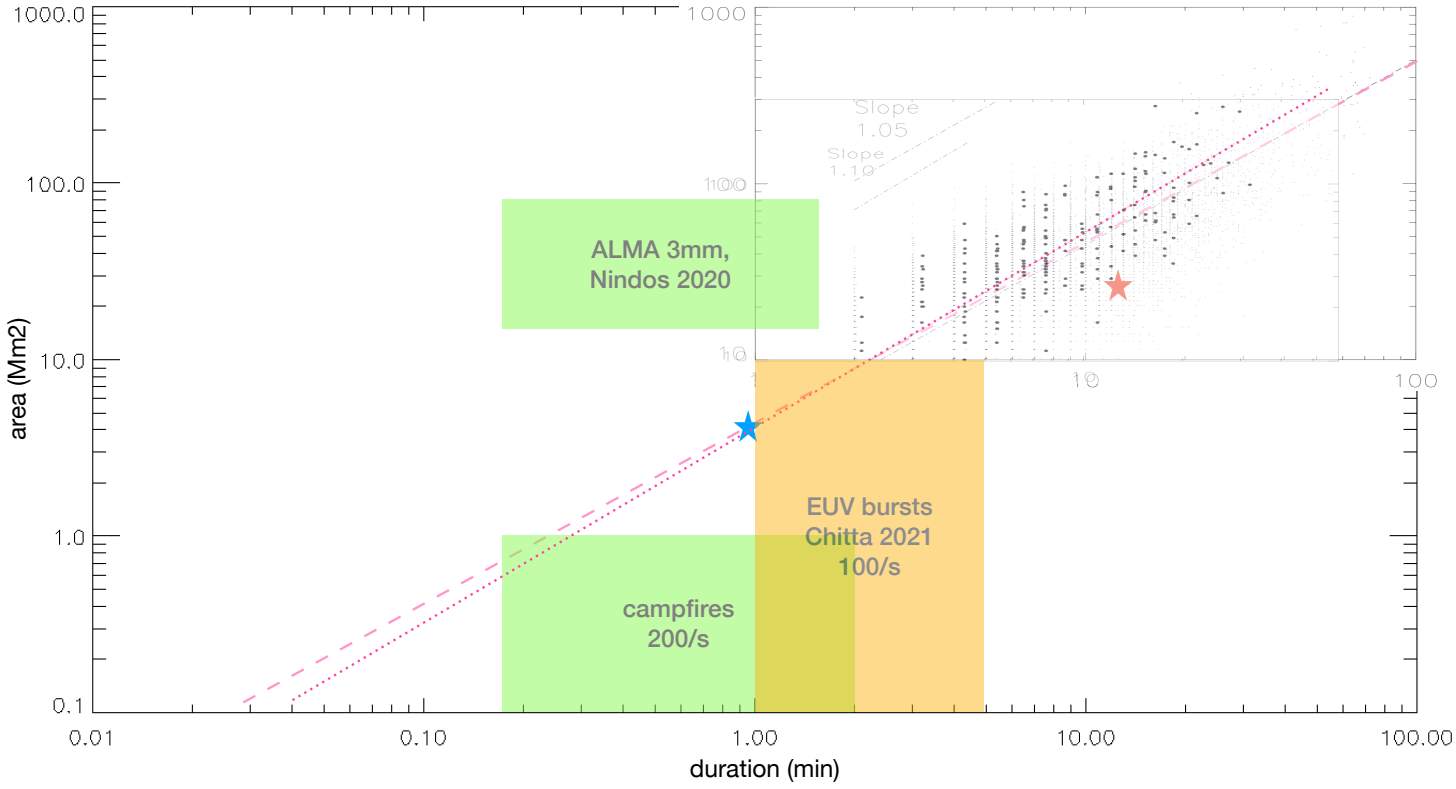

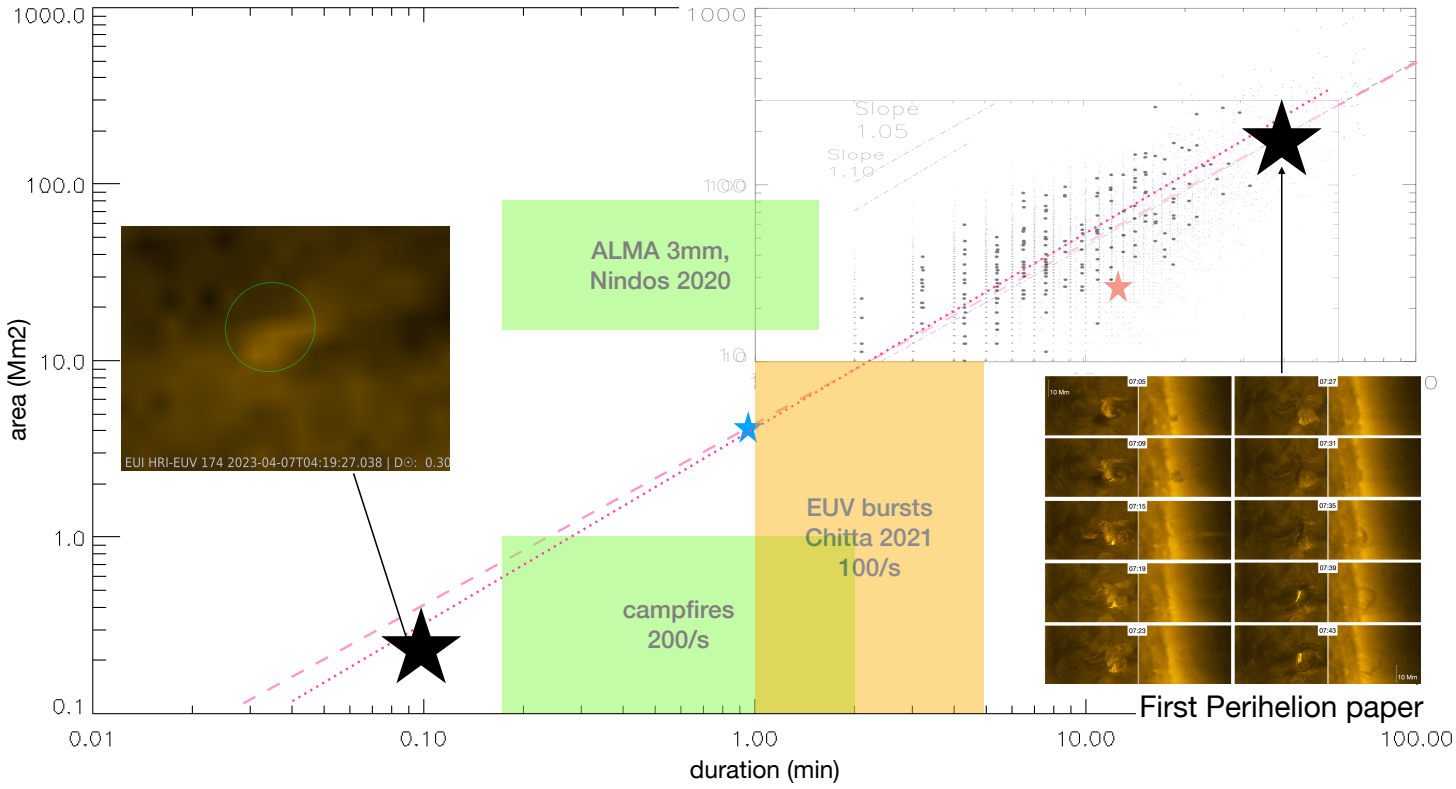

Looking back at EIT brightenings. What is the difference with EUI campfires?

- The various categories of EUV quiet Sun brightenings previously baptised (blinkers, explosive events, EUV burst, campfires) are possible all manifestations of the same family of flare-like energy releases, constrained by the characteristics of the dataset and the instrument that observed it
- EUI has the potential to observe EUV quiet Sun brightenings from the smallest to the largest scales and thereby thus connect the previously observed categories.
- Co-observations with other instruments (radio, spectrographs, etc) will be essential.

Looking back at EIT brightenings. What is the difference with EUI campfires?

D. Berghmans - ROB/SIDC Seminar 2023 Nov 10 Friday 14:30

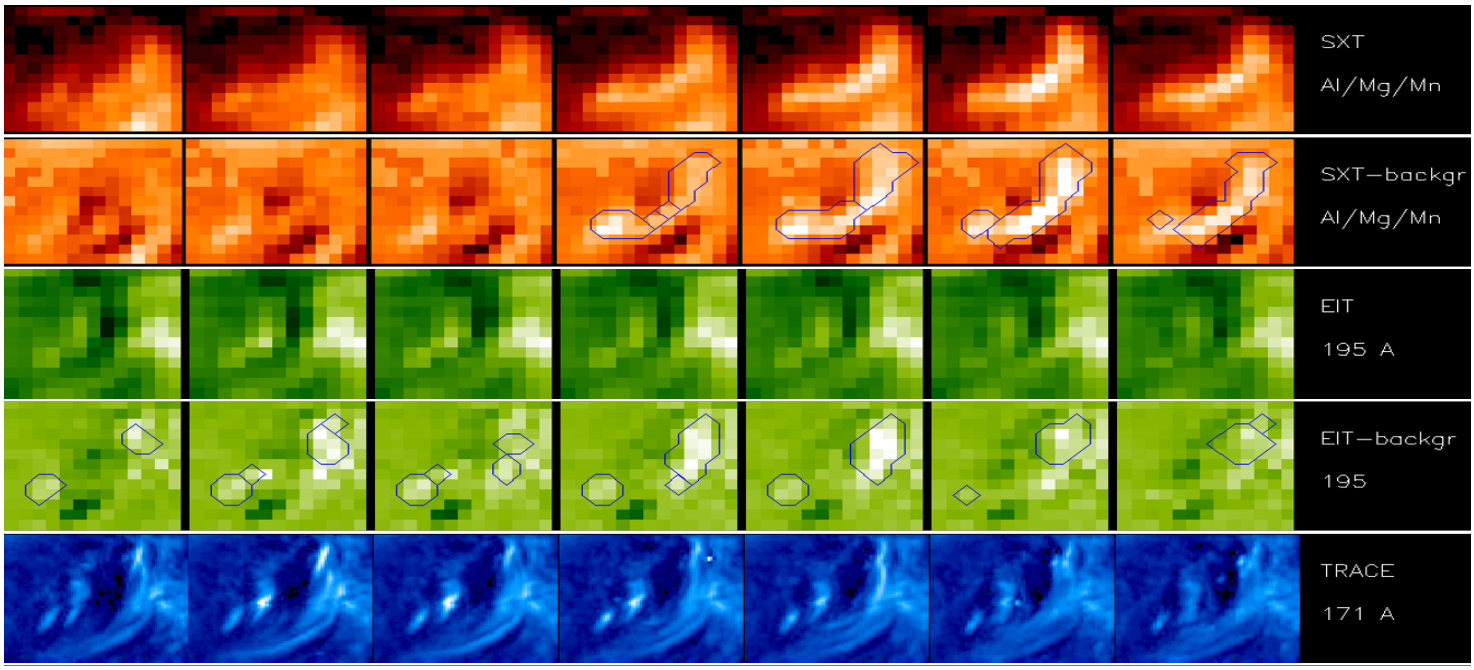

Limits to extrapolation

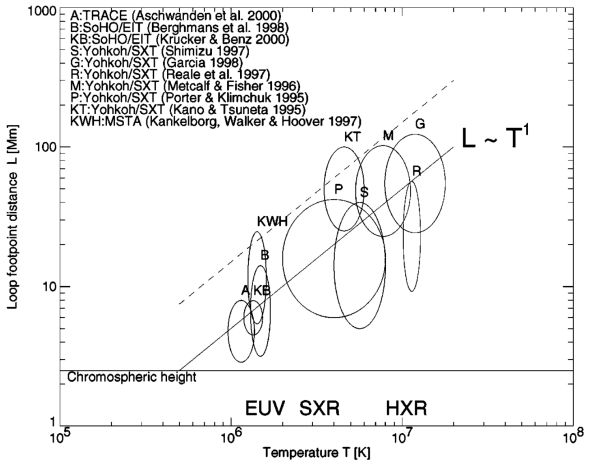

Figure 1. Observed loop footpoint separation distance L as function of temperature T: for EUV brightenings ($T = 1-2$ MK), nonflaring active region loops ($T = 2-8$ MK), SXR transient brightenings ($T = 4-8$ MK), and flares ($T = 6-20$ MK). Note that the average spatial scale L can be fitted with a power-law scaling law $L \sim T^1$ (solid line) within a factor of ≈ 3 (dashed lines).

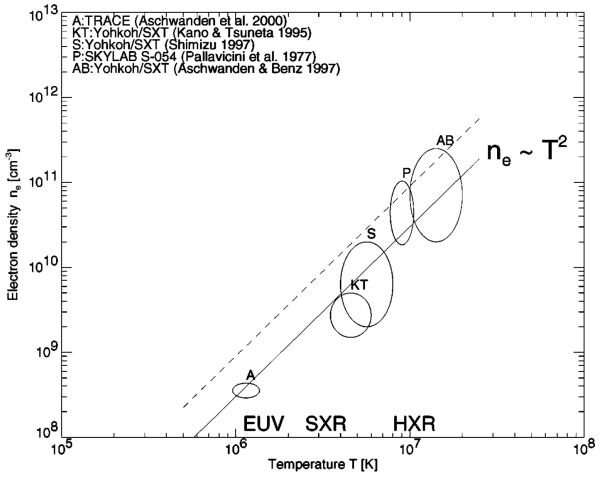

Figure 2. Observed loop electron densities n_e as function of temperature T: for EUV brightenings ($T = 1-2$ MK), transient brightenings ($T = 4-8$ MK), and flares ($T = 6-20$ MK). Note that the average spatial scale L can be fitted with a power-law scaling law $n_e \sim T^2$ (solid line) within a factor of ≈ 3 (dashed lines).

Aschwanden 1999

Limits to extrapolation

Based on this chromospheric pressure limit we predict a lower cutoff of flare loop sizes at $L_{\min} \lesssim 5$ Mm and flare energies $E_{\min} \lesssim 10^{24}$ erg. We show evidence for such a rollover in the flare energy size distribution from recent TRACE EUV data. Based on this energy cutoff imposed by the chromospheric boundary condition we find that the energy content of the heated plasma observed in EUV, SXR, and HXR flares is insufficient (by 2–3 orders of magnitude) to account for coronal heating.

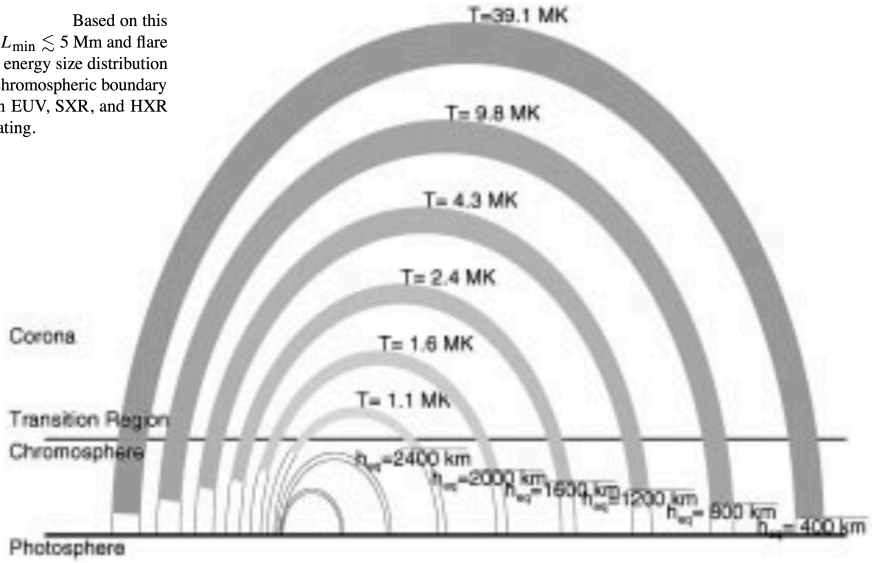

Figure 5. Dependence of the loop volume that is filled with heated plasma (with temperature T) on chromospheric pressure equilibrium height $h_{eq}(T)$. Low-temperature loops are statistically sma according to the scaling law $L(T) \sim T$ and experience pressure balance with the chromosphere higher altitude h_{eq} than high-temperature (statistically larger) loops.

Aschwanden 1999